Membrane model

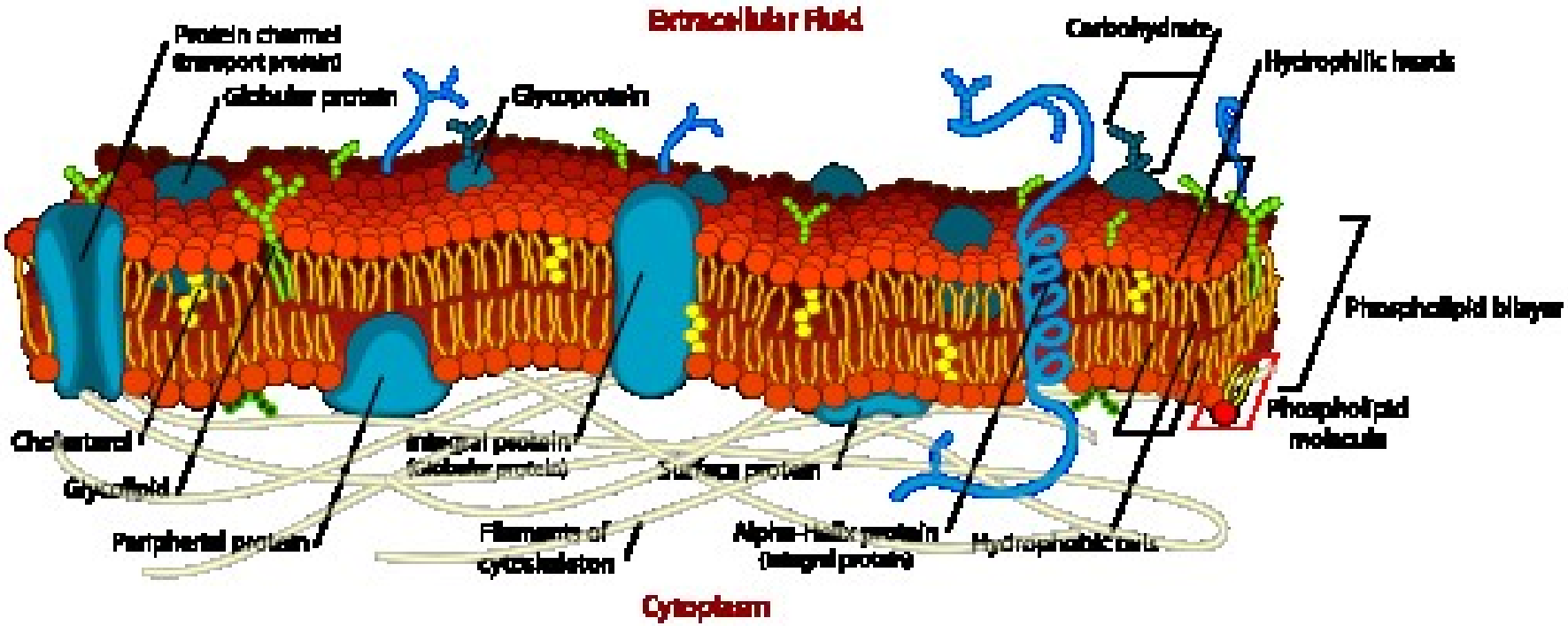

Physical chemical proprieties of gametes membranes.

- Global and local physical and chemical proprieties of cell membrane markedly change, depending on several factors.
- Here we are interested in understanding the effects of temperature, osmotic pressure, and solutes.
- To this aim we need the adoption of models.

L_O and L_D phases in membranes

L_o

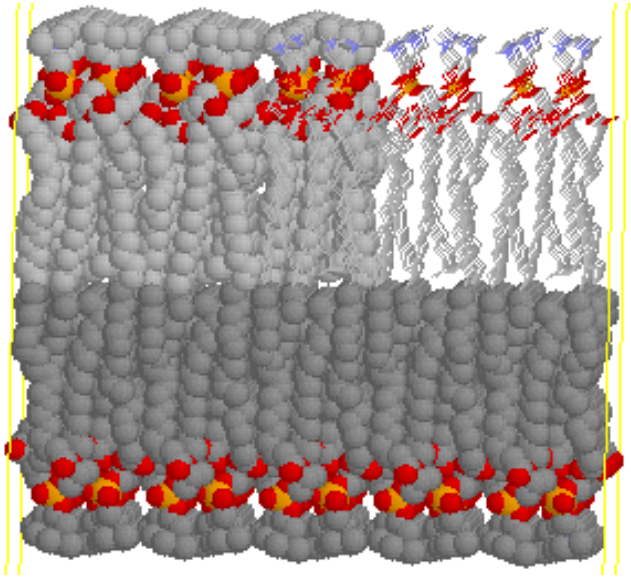

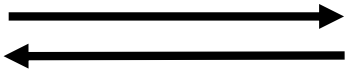

temperature
solutes
…

L_D

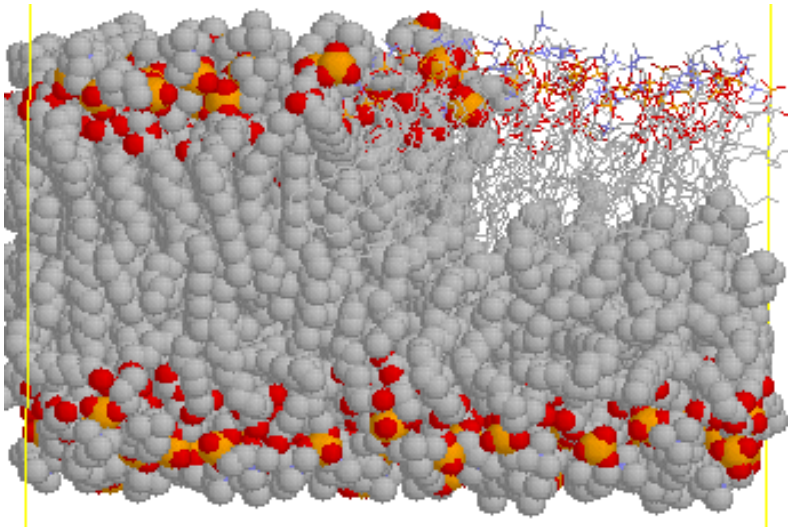

Liquid crystals

Liquid crystals (LCs) are matter in a state that has properties between those of the conventional liquid and those of solid crystal.

Liquid crystals

Classification of condensed matter on the basis of long-range order

	Positional order	Orientational order
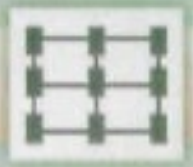 Solid crystal	yes	yes
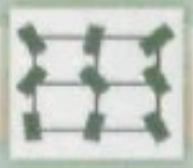 Plastic crystal	yes	no
 Liquid crystal	no	yes
 Isotropic liquid	no	no

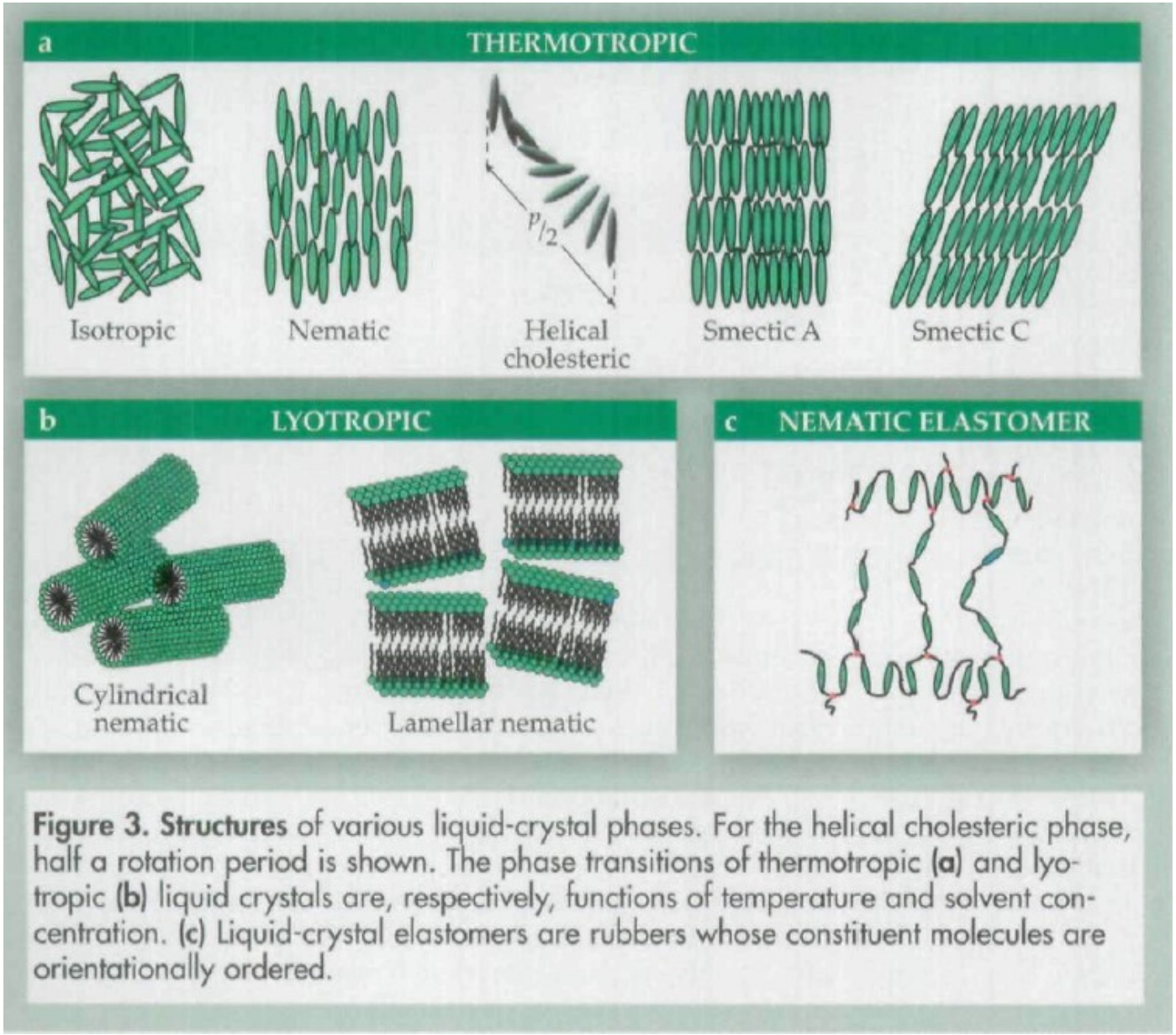

Figure 3. Structures of various liquid-crystal phases. For the helical cholesteric phase, half a rotation period is shown. The phase transitions of thermotropic **(a)** and lyotropic **(b)** liquid crystals are, respectively, functions of temperature and solvent concentration. **(c)** Liquid-crystal elastomers are rubbers whose constituent molecules are orientationally ordered.

Thermotropic liquid crystal

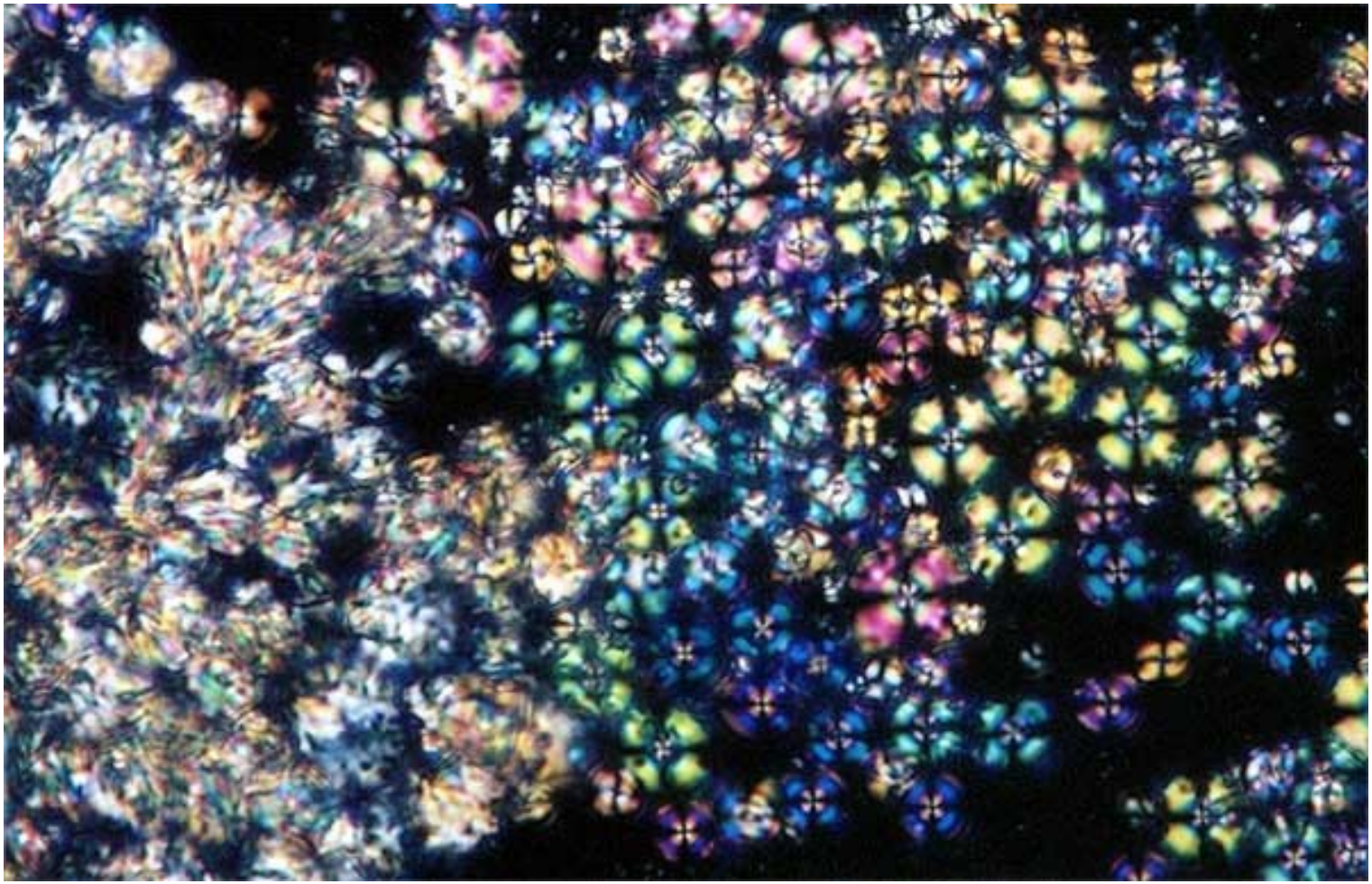

Nematic ⇌ **Smectic**

Lyotropic liquid crystals

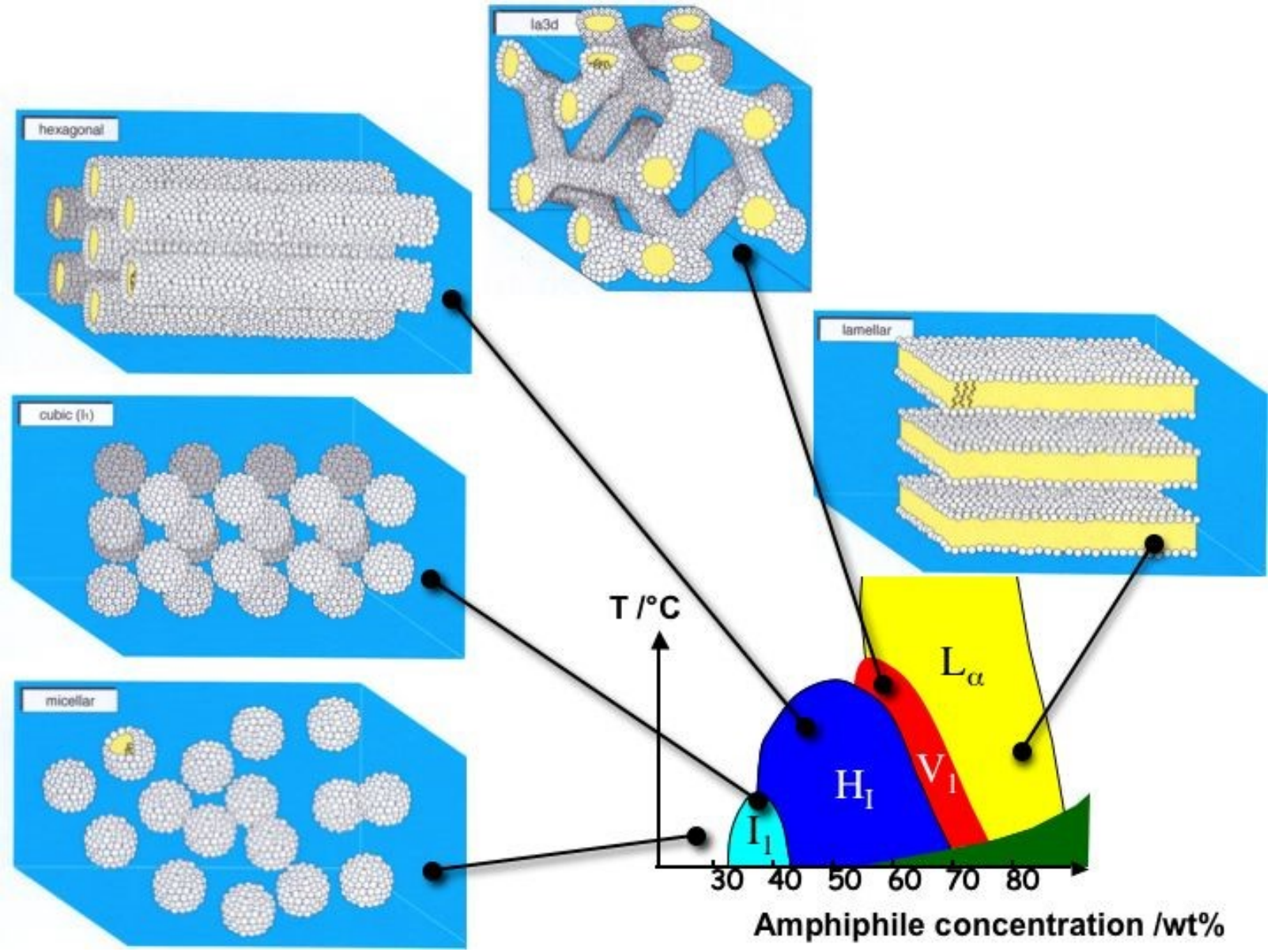

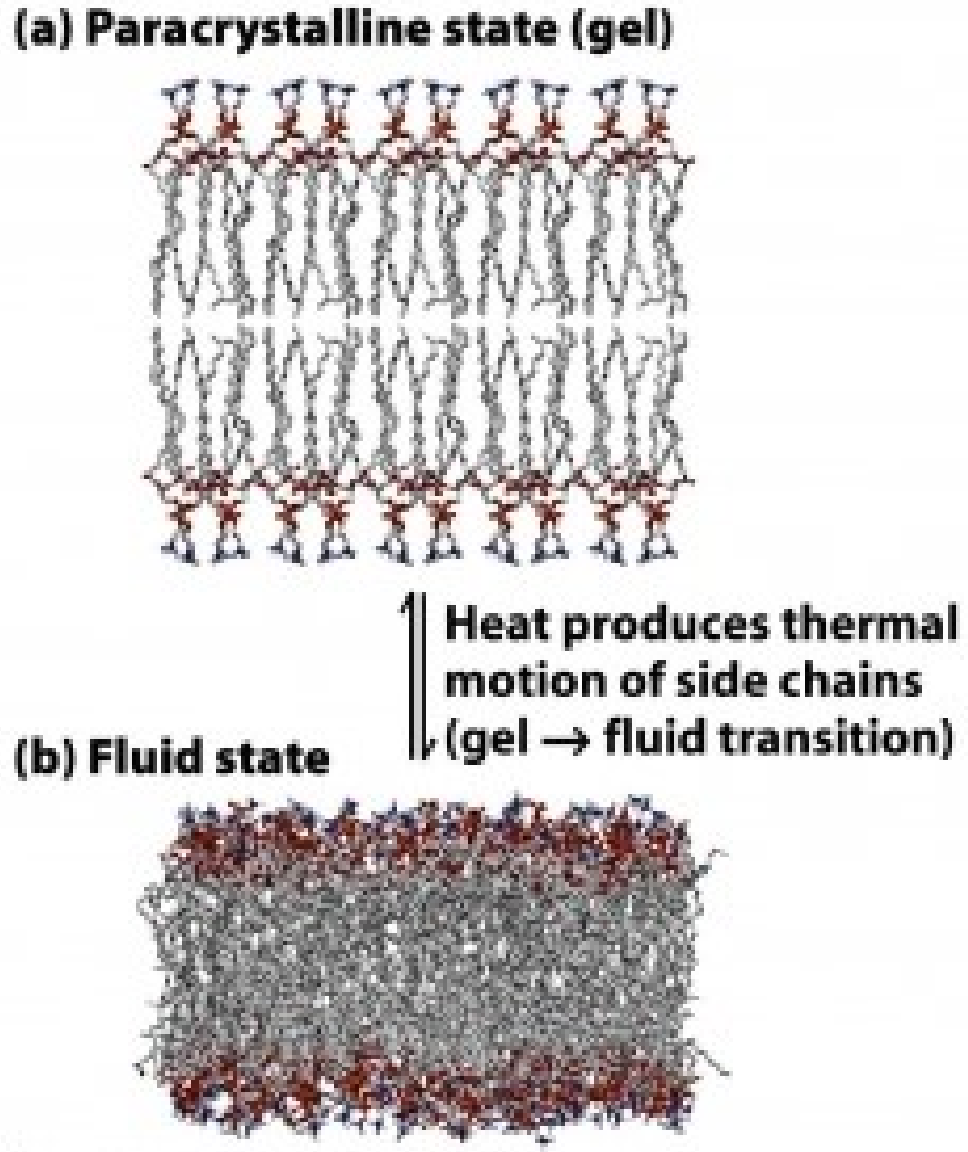

Figure 11-15
Lehninger Principles of Biochemistry, Fifth Edition


Liquid crystals
Thermotropic (heat)
Lyotropic (composition)
Rodlike
Disclike
Lamellar
Hexagonal
Nematic
Smectic
Columnar
Hydrophobic
Hydrophilic

From LCs to cell membranes

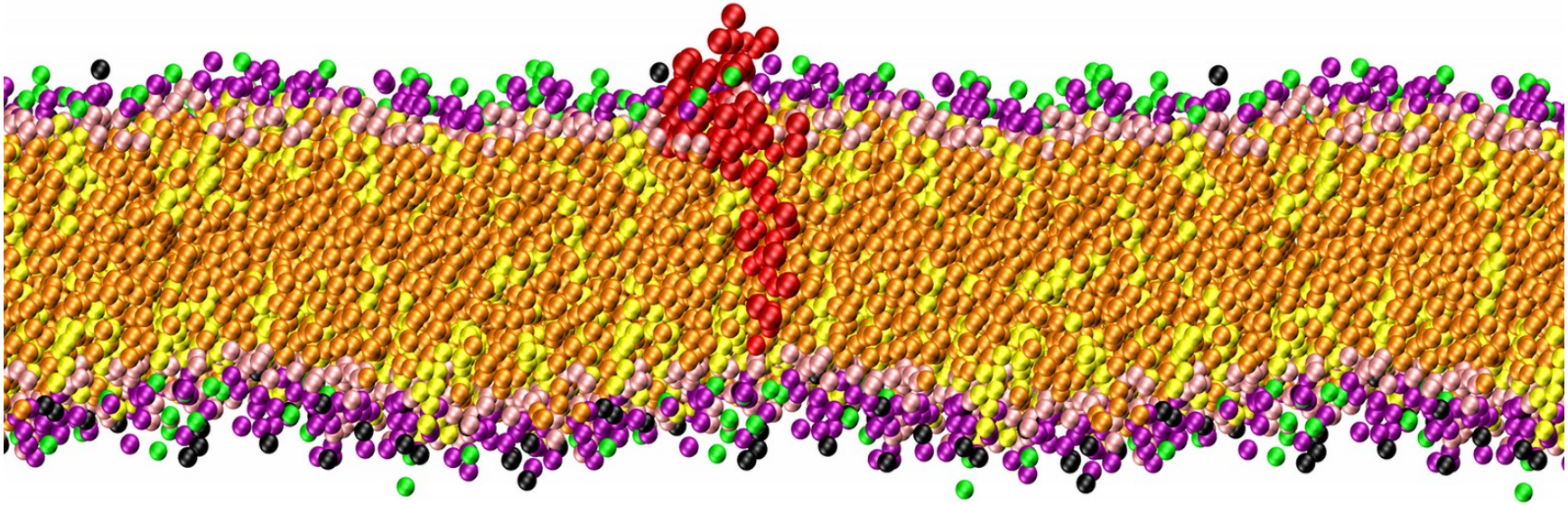

Glycocalyx

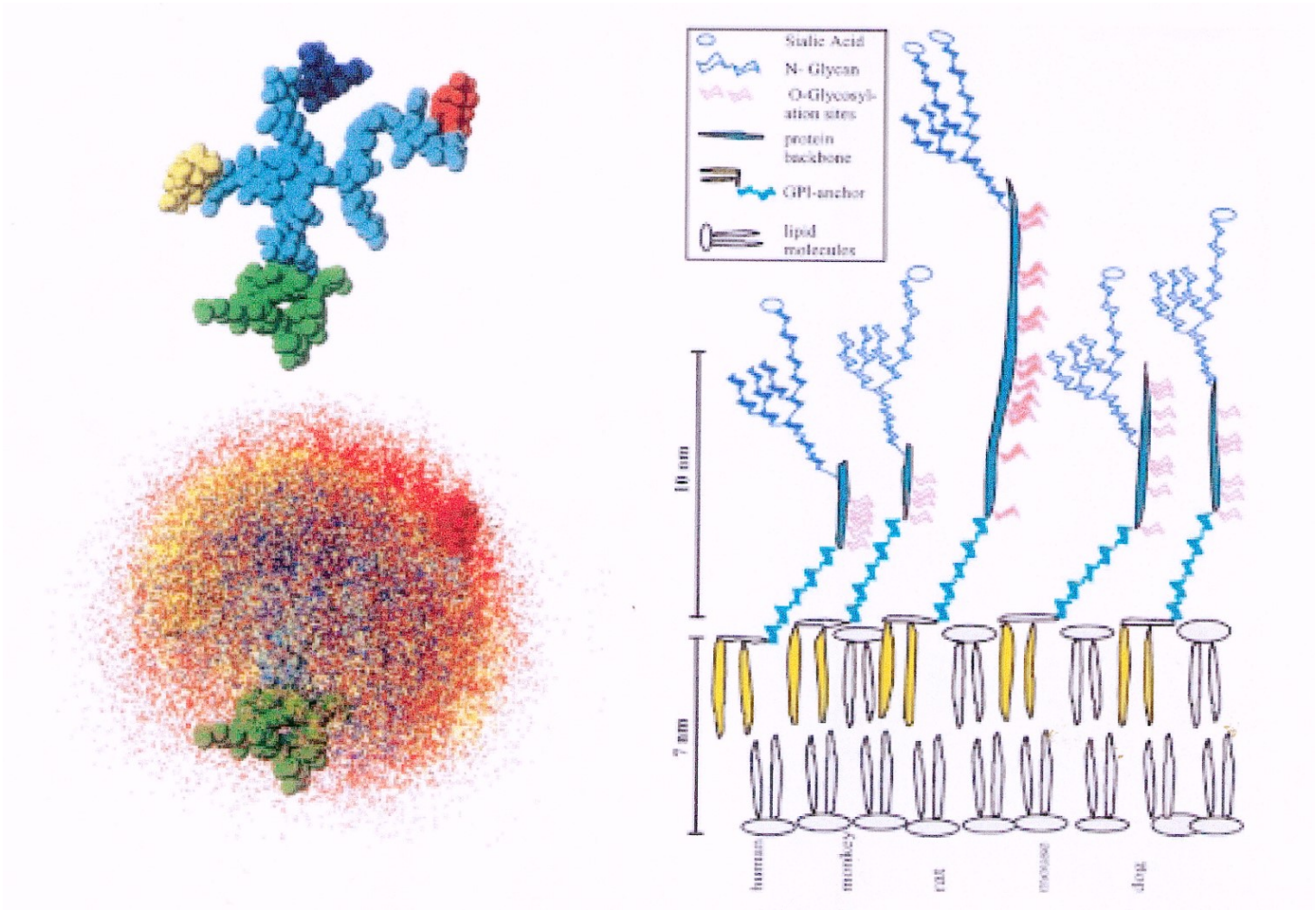
Sialic Acid
N- Glycan
O-Glycosyl-
ation sites
protein
backbone
GPI-anchor
lipid
molecules
10 nm
7 nm
human
monkey
rat
mouse
dog

GLICOCALICE

Table I. Cloned human glycoproteins which bind sequentially to the plasma membrane (PM) of spermatozoa during their transit through the male reproductive tract

Name of cloned glycoprotein	Origin (site of first synthesis)	Size in amino acids (aa) (+ signal peptide, SP) M_r of glycoprotein	Type of glycosylation (consensus sites for N- and O-glycosylation	Sperm domain localization	Proposed functions/comments	Reference
PH-20	testis	455 aa (+35 SP + 19 GPI-anchor SP) 64 kDa	7 N-glycosylation sites >20 O-glycosyl. sites	ejaculated and capacitated spermatozoa: entire head acrosome reacted: IAM→	2 functions: hyaluronidase activity→cumulus penetration IAM-anchored PH-20→secondary binding to zona pellucida	Lin *et al.* (1993)
CD59	testis	103 aa (+25 SP + 22 GPI-anchor SP) 19 kDa	1 N-glycosylation site (verified) 9 O-glycosylation sites	whole sperm surface	protection from complement?	Sawada *et al.* (1990)
SOB1	testis	853 aa 100 kDa	5 N-glycosylation sites 4 O-glycosylation sites	ejaculated spermatozoa: subequatorial	involved in sperm–oocyte binding	Lefèvre *et al.* (1998)
ARP	efferent ducts	230 aa (+19 SP) 30 kDa	1 N-glycosylation site verified by *N*-glycanase F (carbohydrate ≈4 kDa)	postacrosomal on sperm head	involved in fusion of gametes? functional counterpart of rodent AEG	Hayashi *et al.* (1996)
HE2	caput epididymidis	81 aa (+22 SP)	1 N-glycosylation site 6 O-glycosylation sites	ejaculated spermatozoa: acrosomal & equatorial capacitated spermatozoa: mainly equatorial	LRE-motif: cell adhesion?	Osterhoff *et al.* (1994)
HE5	corpus epididymidis	12 aa (+24 SP + 25 GPI-anchor SP)	1 N-glycosylation site (verified) 20–25 kDa	whole sperm surface lesser over chromosome	GPI-anchor: increase in PM stability? carbohydrates: immunosuppression?	Kirchhoff *et al.* (1993)
HE4	cauda epididymidis	95 aa (+30 SP)	1 N-glycosylation site 8 O-glycosylation sites	epididymis: associated to sperm surface lost during capacitation	protease inhibitor?	Kirchhoff *et al.* (1991)

IAM = intra-acrosomal membrane; AEG = acidic epididymal glycoprotein; LRE = Leu-Arg-Glu; GPI = glycosylphosphatidylinositol.

Lipids

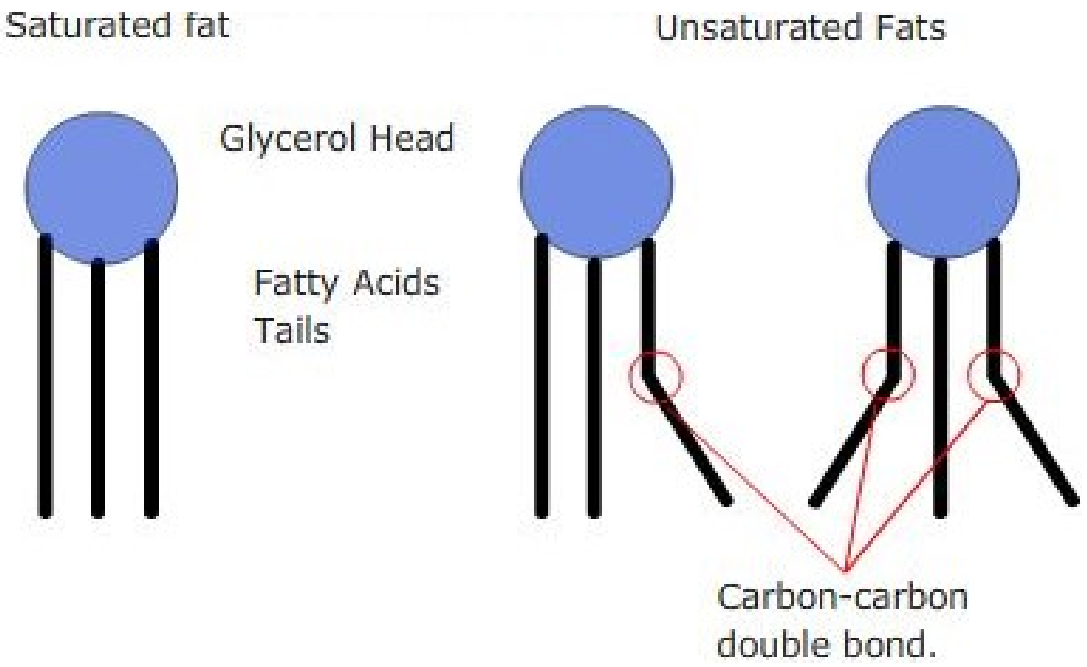
Saturated fat
Unsaturated Fats
Glycerol Head
Fatty Acids
Tails
Carbon-carbon
double bond.

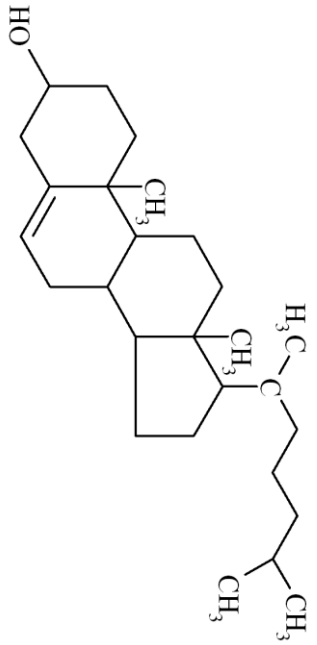
HO
CH3
H3C
CH3
C
CH3
CH3

Tail Length	Double Bonds	Transition Temperature
12	0	-1
14	0	23
16	0	41
18	0	55
20	0	66
22	0	75
24	0	80
18	1	1
18	2	-53
18	3	-60

Transition temperature (in °C) as a function of tail length and saturation. All data are for lipids with PC headgroups and two identical tails.

Lipids chemisty and membrane geometry

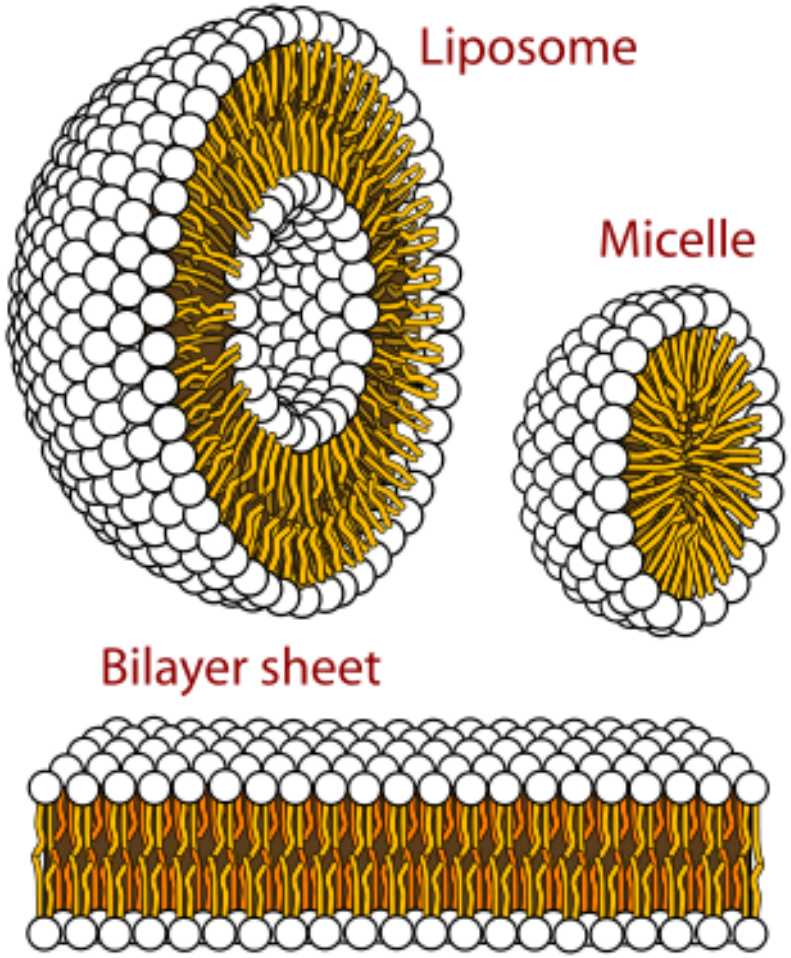

Lipids chemisty and membrane geometry

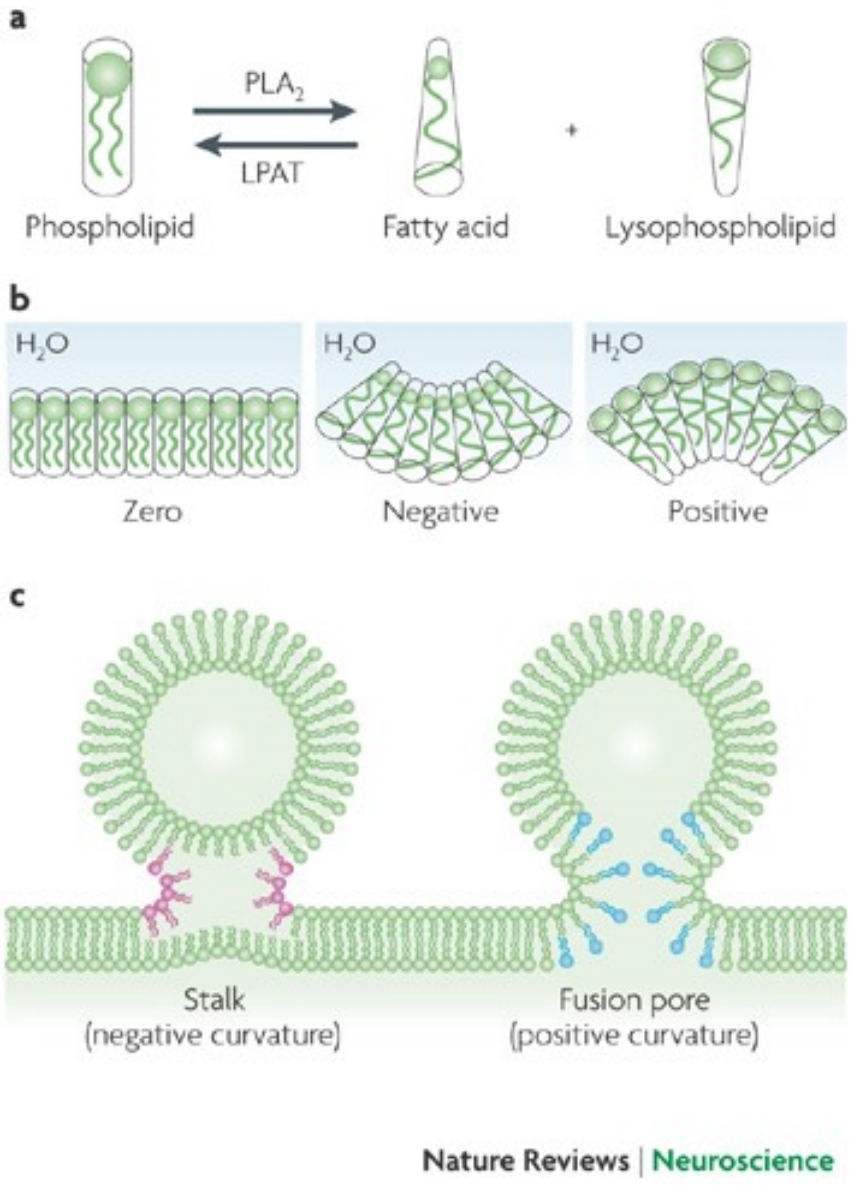

Membrane microdomains

A

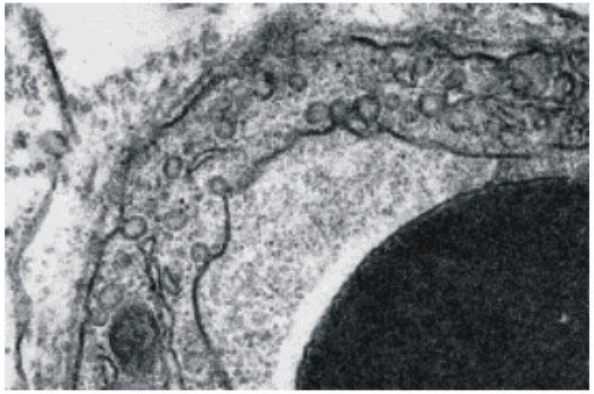

B

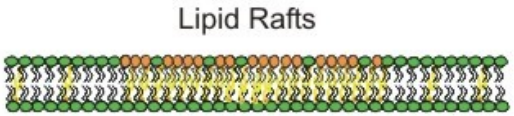

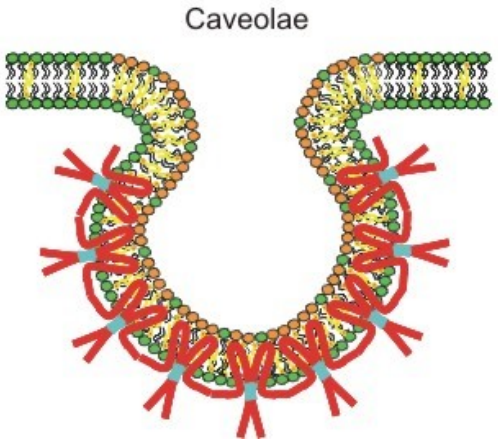

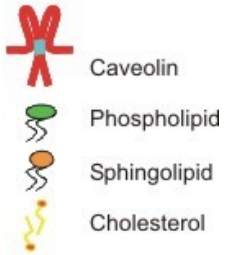

caveolae

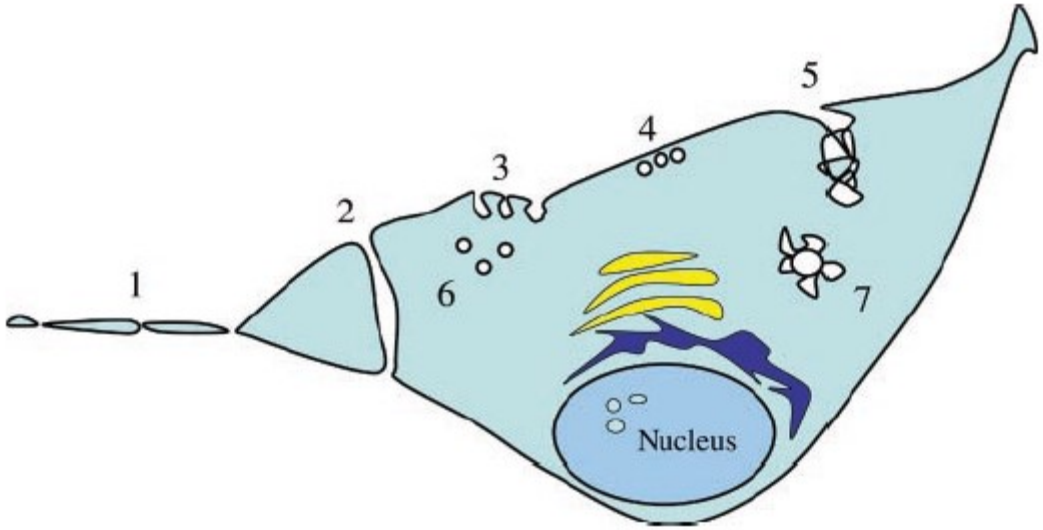

FIG. 1. Stylized view of the cell depicting morphological variants of caveolae and select subcellular compartments. These include *1*) fenstra, *2*) a transcellular channel, *3*) traditional caveolae, *4*) plasmalemmal vesicles (fully invaginated, static caveolae), *5*) a vesiculo-vacuolar organelle (a grapelike cluster of interconnected caveolae and vacuoles), *6*) cavicles (mobile, internalized caveolae not associated with the plasma membrane), and *7*) a caveosome (a slow moving, irregularly shaped, cytoplasmic organelle). Golgi, dark blue; endoplasmic reticulum, yellow.

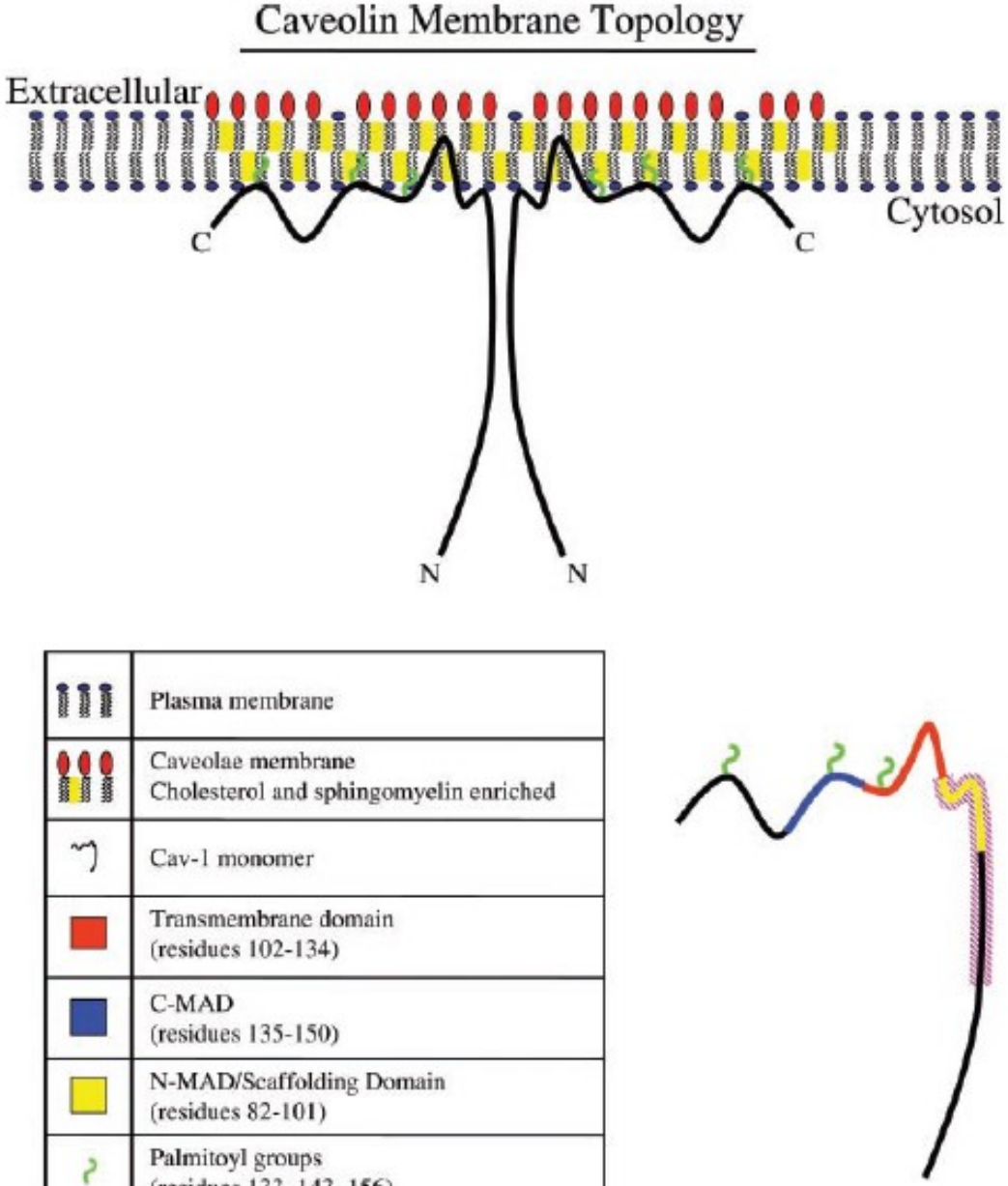

FIG. 6. Caveolin-1 membrane topology and protein domains. In this view, caveolin-1 is depicted as a homodimer for simplicity. Mutational analysis has shown that the C-MAD (blue; residues 135–150) and N-MAD (yellow; residues 82–101) are important for membrane attachment, while the transmembrane domain (red; residues 102–134) is thought to insert into the membrane. Oligomerization is mediated by residues 61–101 (hashed pink). The scaffolding domain (yellow; residues 82–101) recognizes a hydrophobic caveolin-binding motif present within many signaling molecules. Caveolin-1 is also palmitoylated on three conserved cysteine residues (green; 133, 143, and 156). Note that caveolin-1 is not a conventional transmembrane protein. It is thought to have a unique hairpin topology, with no exposure to the extracellular environment.

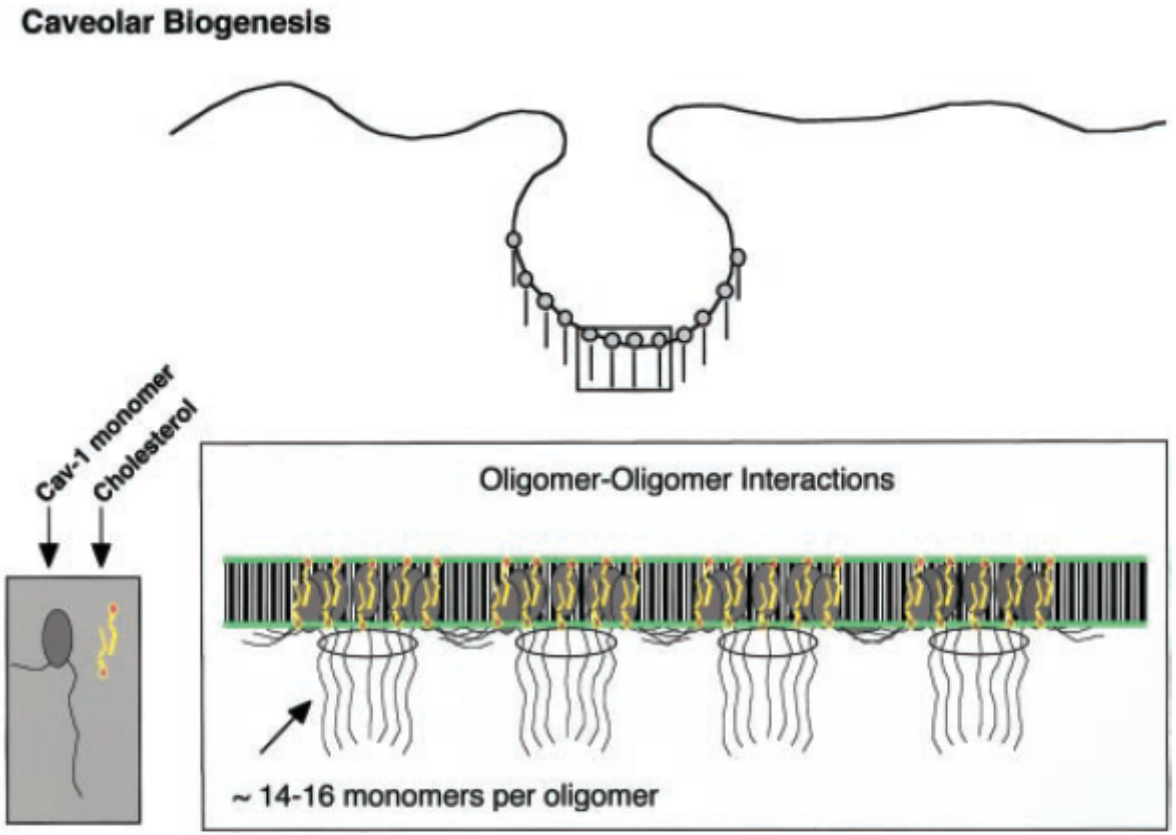

FIG 5. Caveolin-1 oligomerization and caveolae biogenesis. At the level of the ER, caveolin-1 self-associates to form high molecular mass homo-oligomers that contain ~14 to 16 individual caveolin-1 molecules. These caveolin-1 oligomers represent the functional assembly units of caveolae. Then, these caveolin-1 homo-oligomers undergo a second stage of oligomerization during transport to the plasma membrane, most likely at the level of the *trans*-Golgi. In this second stage of oligomerization, individual caveolin-1 oligomers interact with each other via their C-terminal domains, forming an extensive network or meshwork on the underside of the plasma membrane. This large meshwork of oligomers may act synergistically with cholesterol (yellow) to distort the membrane and to drive the invagination of caveolae.

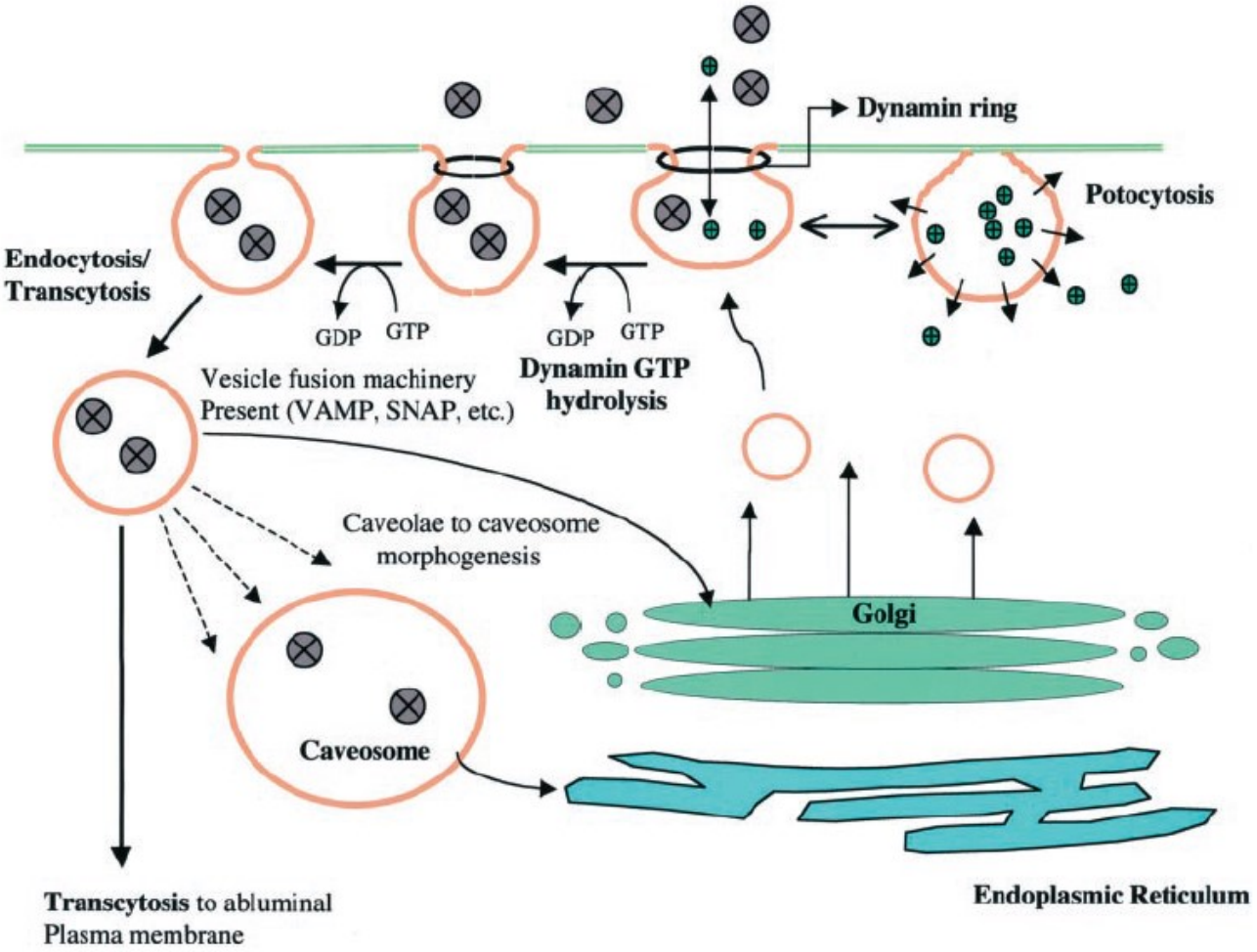

FIG 6. Caveoale vesicular trafficking: transcytosis, endocytosis, and potocytosis. Caveolae appear to mediate the selective uptake and transport of several molecules via different processes (transcytosis, endocytosis, and potocytosis). In transcytosis, caveolae transport proteins from the luminal side of the endothelial cell to the interstitial compartment for subsequent uptake by underlying tissues. In caveolae-mediated endocytosis (distinct from that of clathrin-coated pits), caveolae bud off from the plasma membrane and fuse with various intracellular compartments. Possible transport routes include the recently characterized caveolae-caveosome-ER pathway. In potocytosis, caveolae mediate the uptake of small solutes (<1 kDa) by pinching off but remaining associated with the plasma membrane. The molecular machinery involved in this caveolar fission/fusion is the same as that used for numerous other vesicular transport processes with requirements for dynamin, VAMP, SNAP-25, the SNARE complex, and GTP hydrolysis.

Signaling in caveole

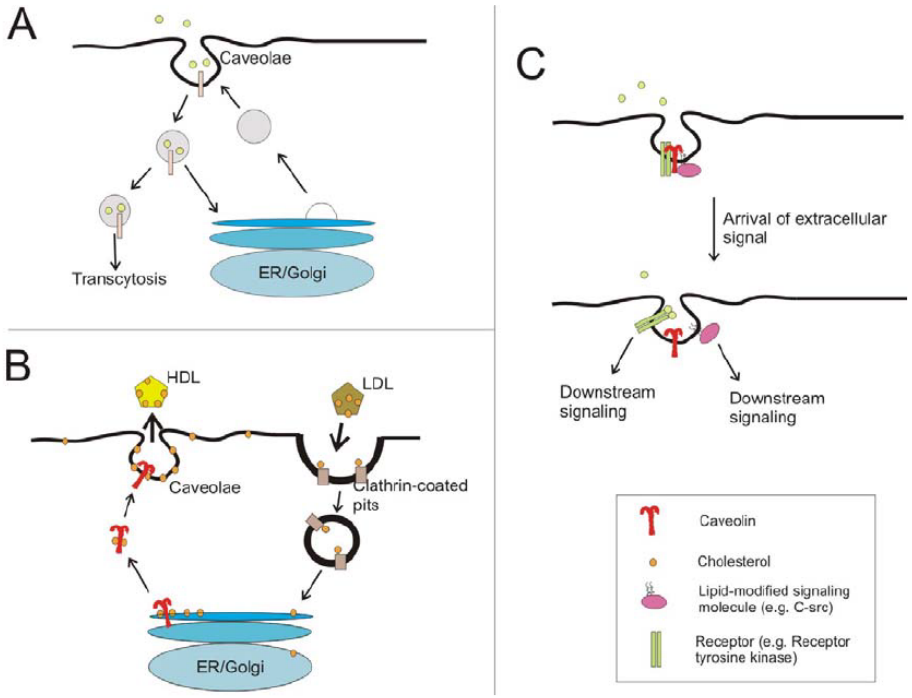

Figure 2. Proposed functions of caveolae and the caveolins (adapted from (Razani and Lisanti, 2001))
A) Certain molecules have been shown to be predominantly endocytosed via caveolae and not clathrin-coated vesicles. The fate the cargo in a fully invaginated caveola is not entirely understood; however, there is evidence to suggest that depending on the cell type, caveolae can deliver their contents to the ER/golgi compartments or to the abluminal side of a cell.
B) Intracellular cholesterol is thought to be transported to plasma membrane caveolae via a golgi-independent caveolin-mediated route. Caveolae then can serve as "relay stations" to deliver the membrane cholesterol to the bulk plasma membrane or to cholesterol-transporters such as HDL particles.
C) Caveolae are now thought to act as signalosomes, or entities in which signal transduction events can take place efficiently. A higher level of regulatory complexity is provided by the caveolins where signaling molecules can be bound until extracellular ligands relieve them of inhibition. Here, the dynamic regulation of a receptor tyrosine kinase (e.g. EGF receptor) and a lipid-modified kinase (e.g. the src-tyrosine kinase) in caveolae are shown.

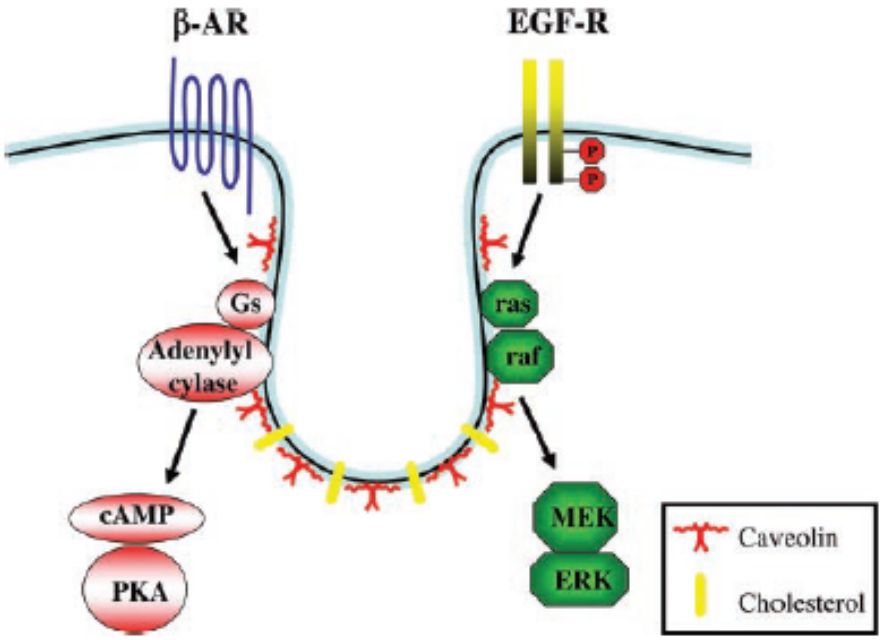

FIG. 8. Signaling through caveolae. In this view, two separate receptors are shown docking with a cholesterol and caveolin-enriched caveola organelle, following ligand-mediated stimulation. The β-adrenergic receptor (β-AR; blue) is a conventional G protein-coupled receptor with seven membrane-spanning domains. When stimulated, this receptor initiates a signaling cascade conveyed through several caveolae-localized proteins, beginning with the activation of G_s subunits. This, in turn, leads to the activation of adenylyl cyclase, which increases intracellular cAMP concentrations, resulting in the activation of protein kinase A (PKA). On the *right*, an activated epidermal growth factor receptor (EGF-R) is also shown docking with the caveola, leading to the activation of a proliferative pathway involving several caveolae-associated proteins of the p42/44 mitogen-activated protein kinase cascade (Ras/Raf/MEK/ERK).

rafts

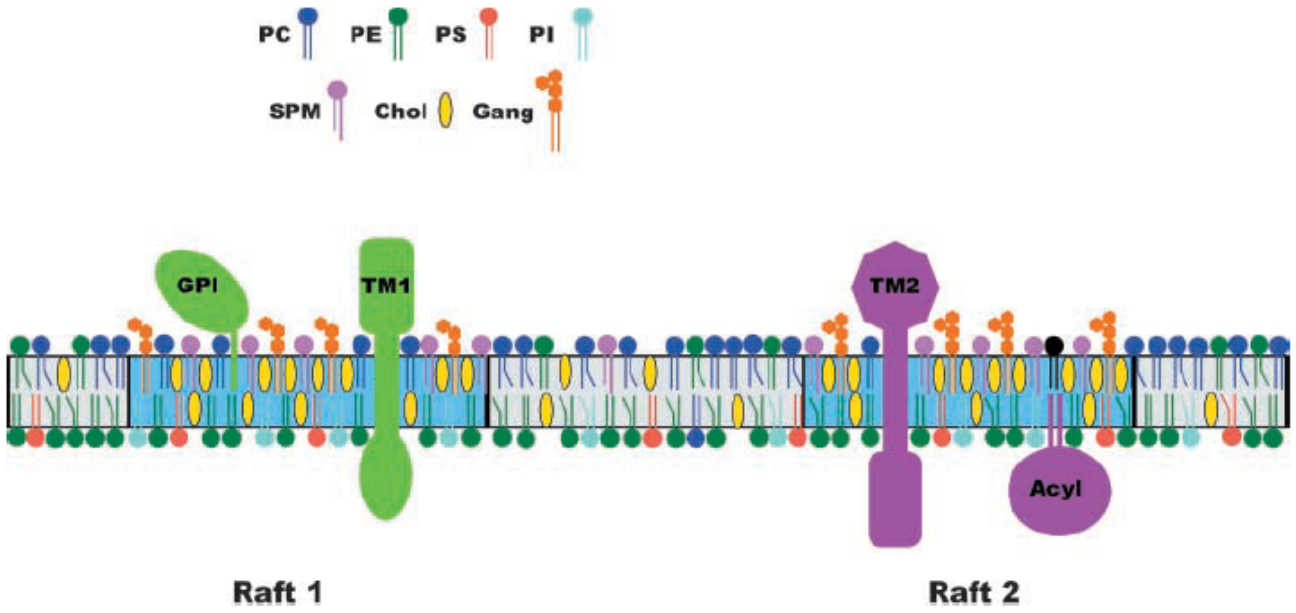

Fig. 1. Structure of lipid rafts. Lipid rafts (blue bilayer) are specialized membrane domains containing high concentrations of cholesterol, sphingomyelin, and gangliosides. They are also enriched in phospholipids that contain saturated fatty acyl chains (straight lines in lipid tails). This composition results in lateral phase separation and the generation of a liquid-ordered domain. Bulk plasma membrane (gray) contains less cholesterol, sphingomyelin, and gangliosides, and more phospholipids with unsaturated acyl chains. As a result, it is more fluid than lipid rafts. A variety of proteins partition into lipid rafts: glycosylphosphatidylinositol-anchored proteins; transmembrane proteins (TM); dually acylated proteins (Acyl). As shown in the diagram, not all lipid rafts have the identical protein or lipid composition (Raft 1 vs. Raft 2). Not shown are invaginated caveolae, a subclass of lipid rafts that contains caveolin. PC, phosphatidylcholine; PE, phosphatidylethanolamine; PS, phosphatidylserine; PI, phosphatidylinositol, SPM, sphingomyelin, Chol, cholesterol; Gang, gangliosides.

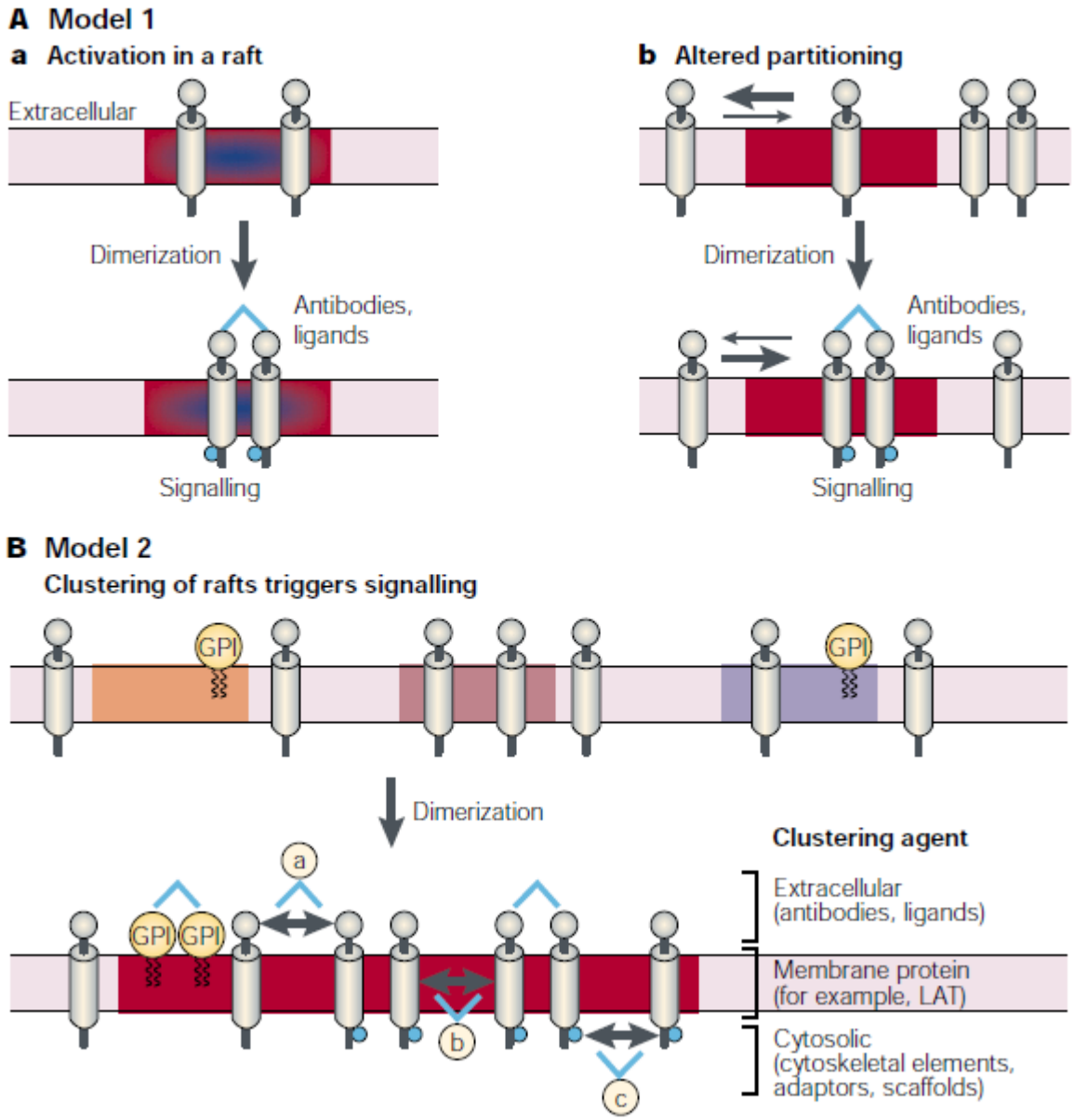
A Model 1
a Activation in a raft
Extracellular
Dimerization
Antibodies, ligands
Signalling
b Altered partitioning
Dimerization
Antibodies, ligands
Signalling
B Model 2
Clustering of rafts triggers signalling
GPI
GPI
Dimerization
a
GPI
GPI
b
c
Clustering agent
Extracellular (antibodies, ligands)
Membrane protein (for example, LAT)
Cytosolic (cytoskeletal elements, adaptors, scaffolds)

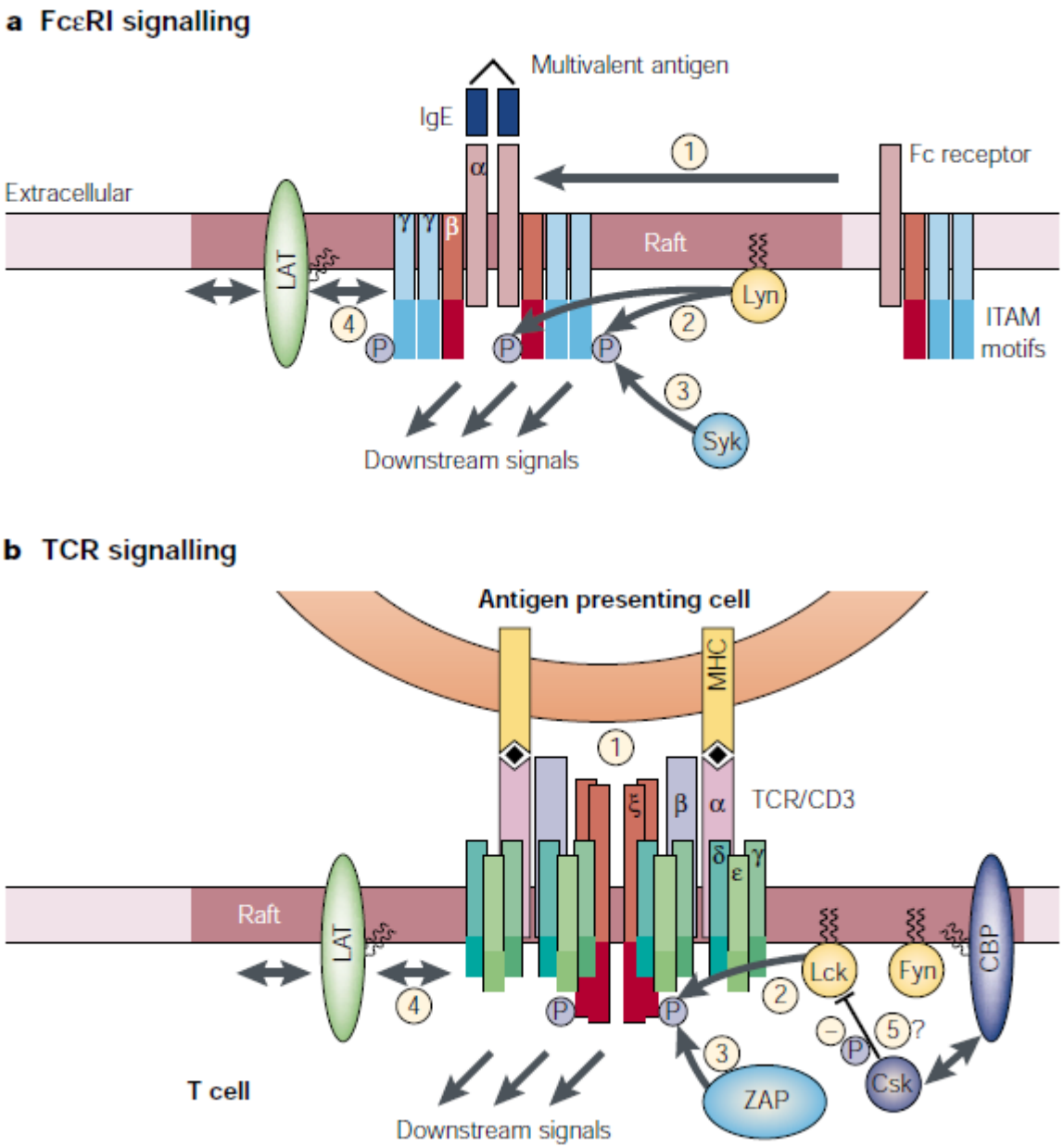
a FcεRI signalling
Multivalent antigen
IgE
α
1
Fc receptor
Extracellular
γ
γ
β
Raft
LAT
Lyn
4
2
ITAM
motifs
P
P
P
3
Syk
Downstream signals
b TCR signalling
Antigen presenting cell
MHC
1
ξ
β
α
TCR/CD3
δ
ε
γ
Raft
LAT
Lck
Fyn
CBP
4
2
P
P
5?
−
P
3
Csk
ZAP
T cell
Downstream signals

Membranes fusion

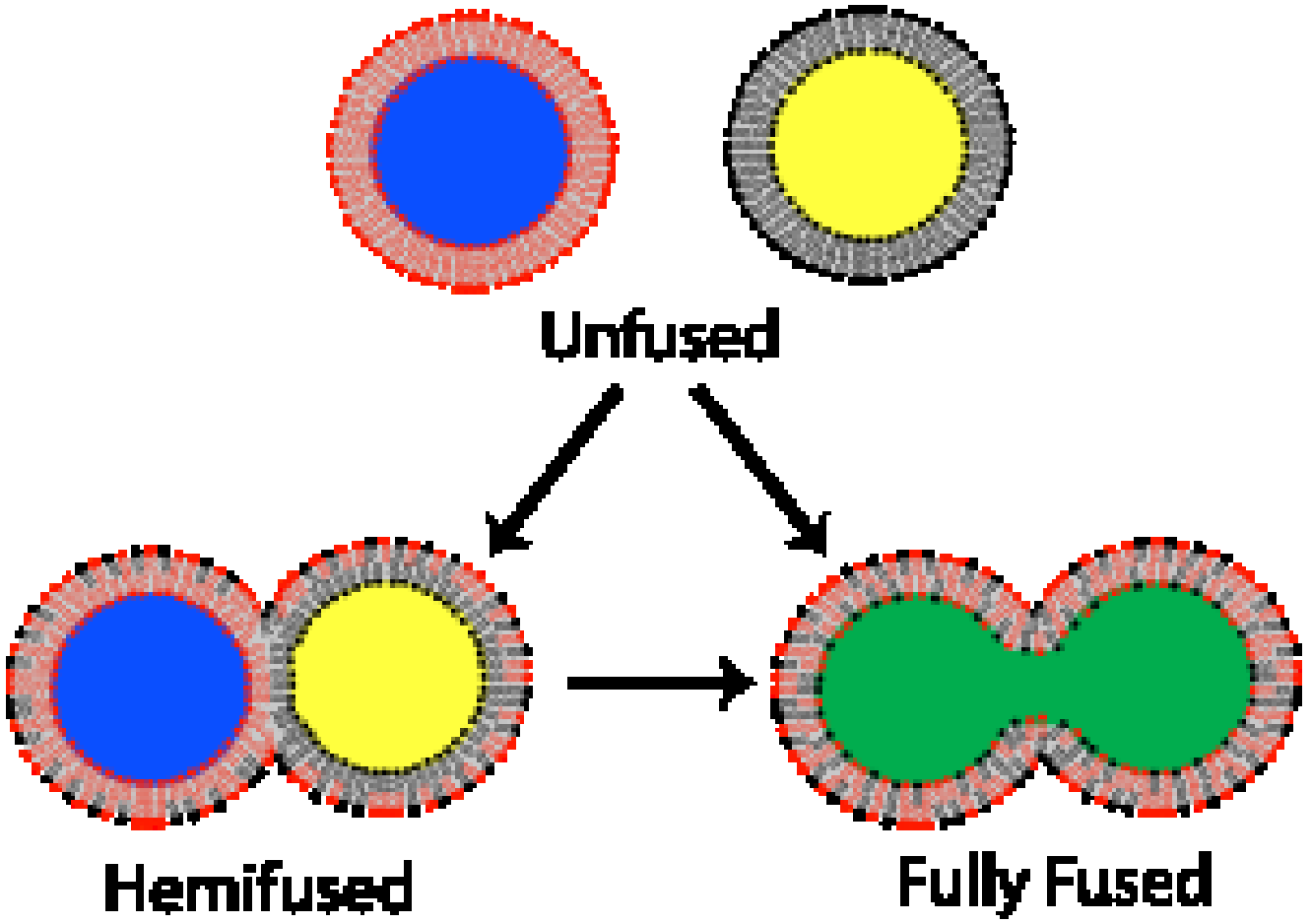

STEPS

1) the two bilayers become closer (nM).
2) The two bilayers come in contact (Å): to allow the to bylaiers come so close, the water molecules that hydrate the hydrophilic heads of lipids need to be removed.
3) Onset of a nucleation.
4) From the nucleation the fusion extends and the components of the two bilayers fuse.

What forces are involved?

1) **Hydration repulsion**: As water molecules have an affinity towards hydrophilic head groups, they try to arrange themselves around the head groups of the lipid molecules and it becomes very hard to separate this favorable combination.

The potential V_R is given by

$$V_R = C_R \cdot \exp\left[\frac{-z}{\lambda_R}\right]$$

C_R (>0) = measure of the hydration interaction energy for hydrophilic molecules of the given system,

λ_R = characteristic length scale of hydration repulsion,

z = the distance of separation.

2) **Hydrophobic attraction**: they are the attractive entropic forces between two hydrophobic groups in aqueous media, e.g. between two long hydrocarbon chains in aqueous solutions. The magnitude of these forces depends on the hydrophobicity of the interacting groups as well as the distance separating them. The physical origin of these forces is a debated issue but they have been found to be long-ranged and are the strongest among all the physical interaction forces operating between biological surfaces and molecules. They are responsible for rapid coagulation of hydrophobic particles in water and play important roles in various biological phenomena including folding and stabilization of proteins and fusion of cell membranes.

The potential V_A is given by

$$V_A = C_A \cdot \exp\left[\frac{-z}{\lambda_A}\right]$$

C_A (<0) = the hydrophobic interaction energy for the given system

λ_A is a characteristic length scale of hydrophobic attraction

z = is the distance of separation

3) **Forze di van der Waals**: These forces arise due to dipole-dipole interactions between molecules of bilayers. As molecules come closer, this attractive force arises due to the ordering of these dipoles.

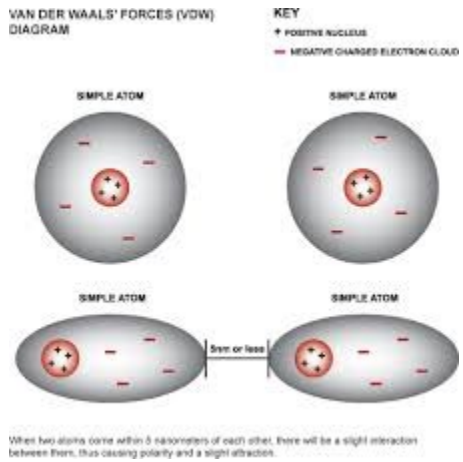

In bilayers, the the van der Waals interaction potential V_{VDW} is given by

$$V_{VDW} = -\frac{H}{12\pi} * \left(\frac{1}{z^2} - \frac{2}{(z+D)^2} + \frac{1}{(z+2D)^2} \right)$$

H = costante di Hamaker,

D = spessore del bilayer

z = distanza tra I bilayer

- When two bilayers become closer the repulsive force due to hydration repulsion predominates.
- Once the fusion starts, the hydrophobic tails of membrane lipids are exposed and the hydrophobic attraction become crucial.
- The van der Waals forces do not seem to have important effects on the membrane fusion process.

1)

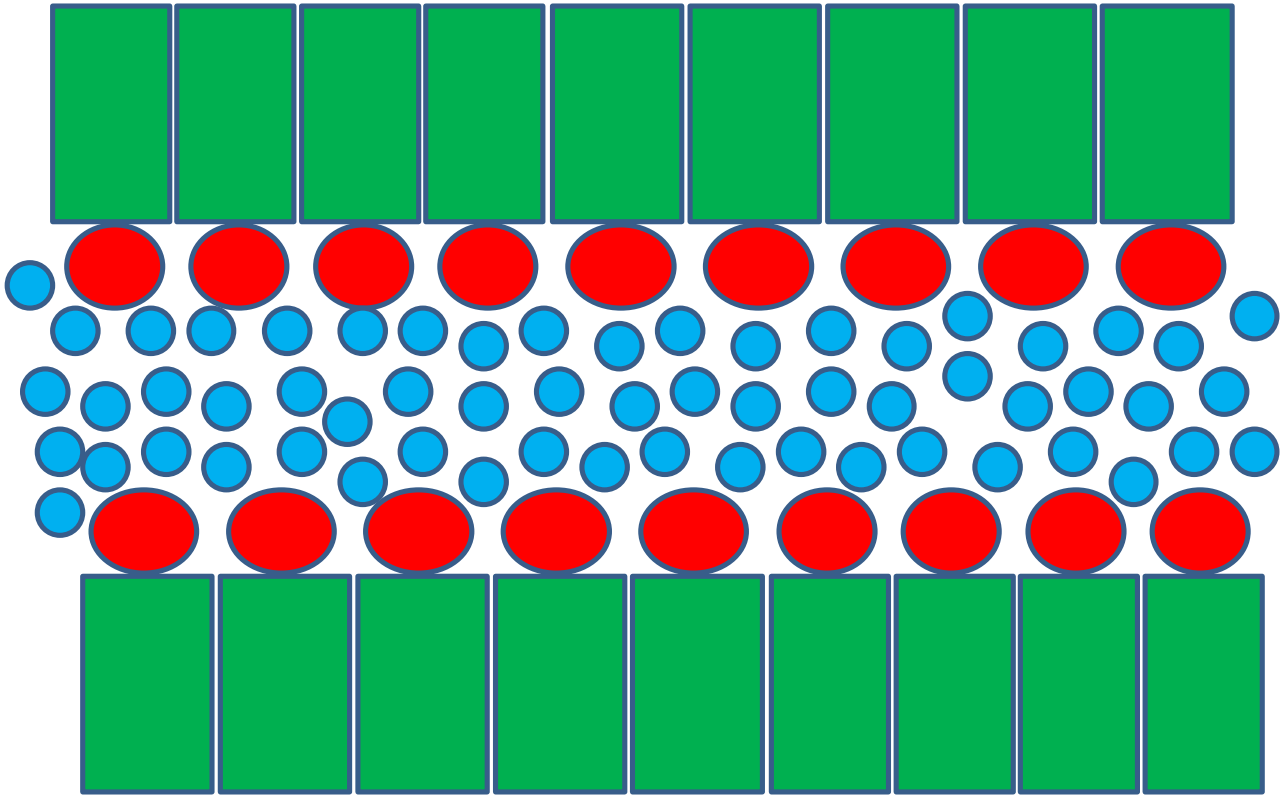

2)

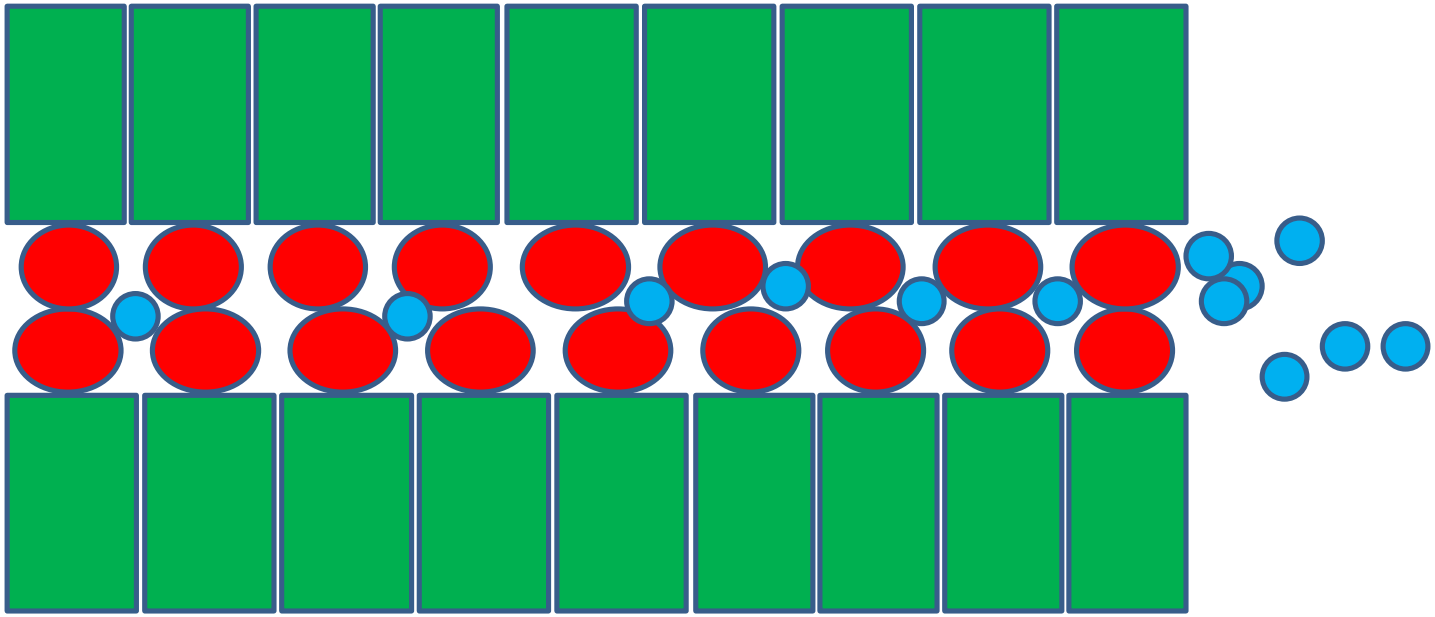

3)

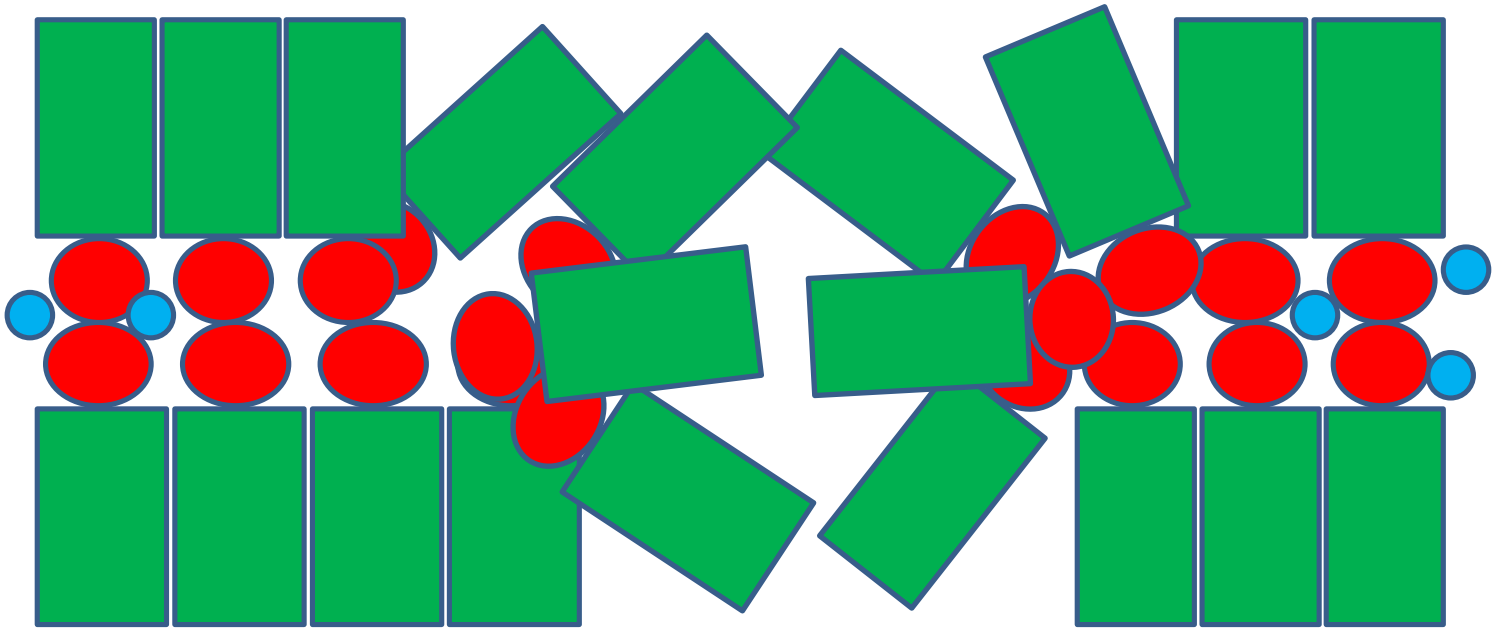

4)

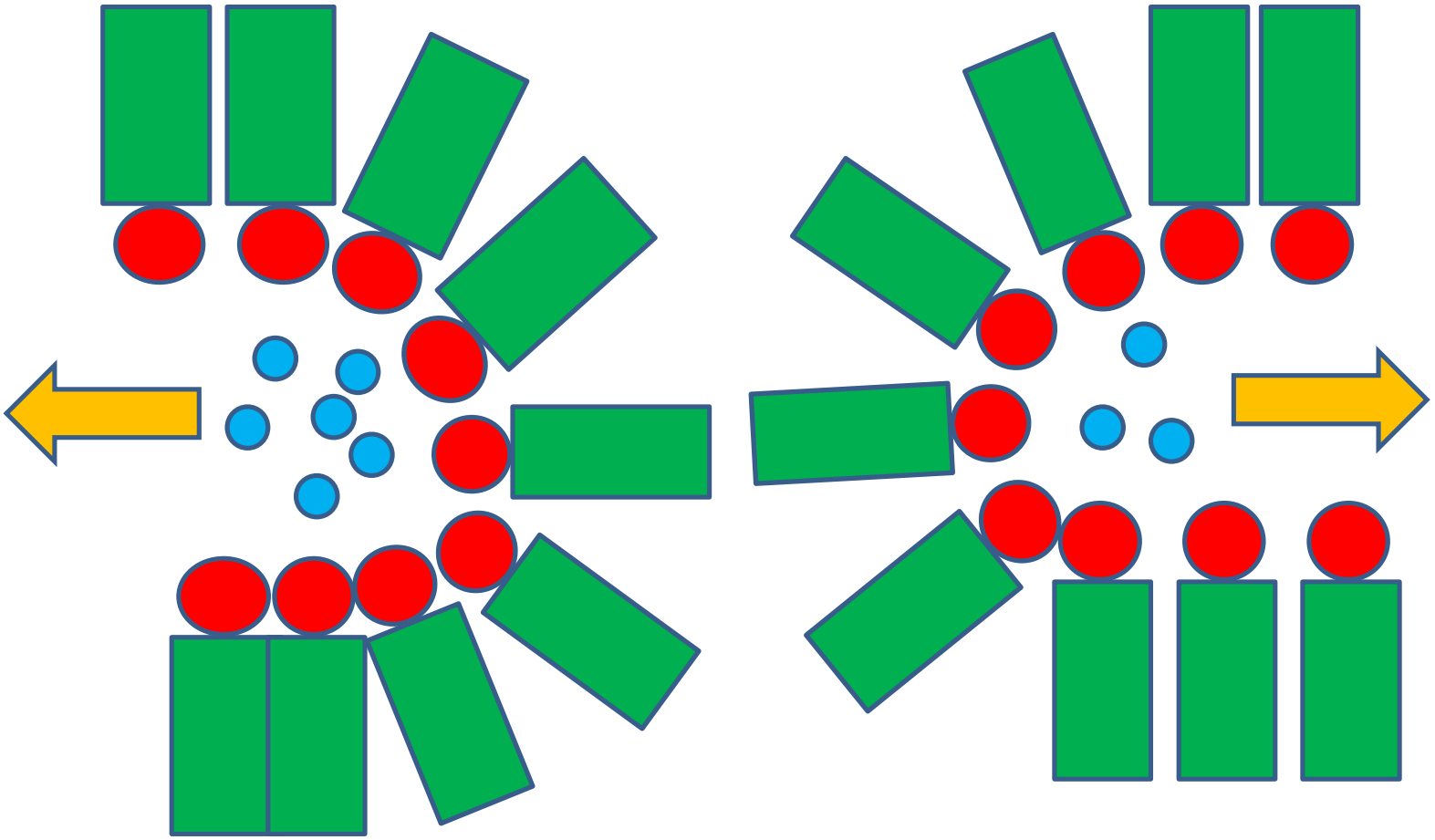

Lipids chemisty and membrane fusion

- Lipid head:as the head is charged, most strongly it binds water and the greater is the hydrophilic repulsion force.
- A small head facilitates the formation of 3D geometries.

Phosphotidylethonlamine (PE)

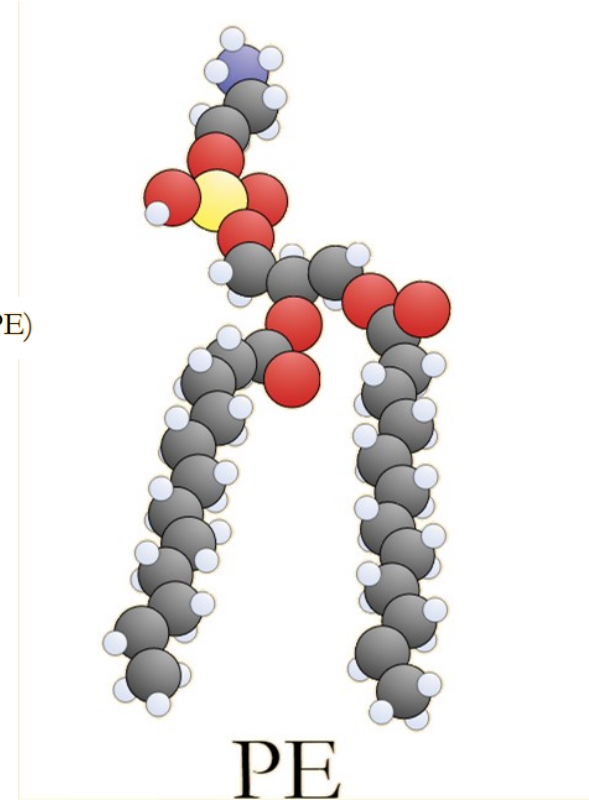

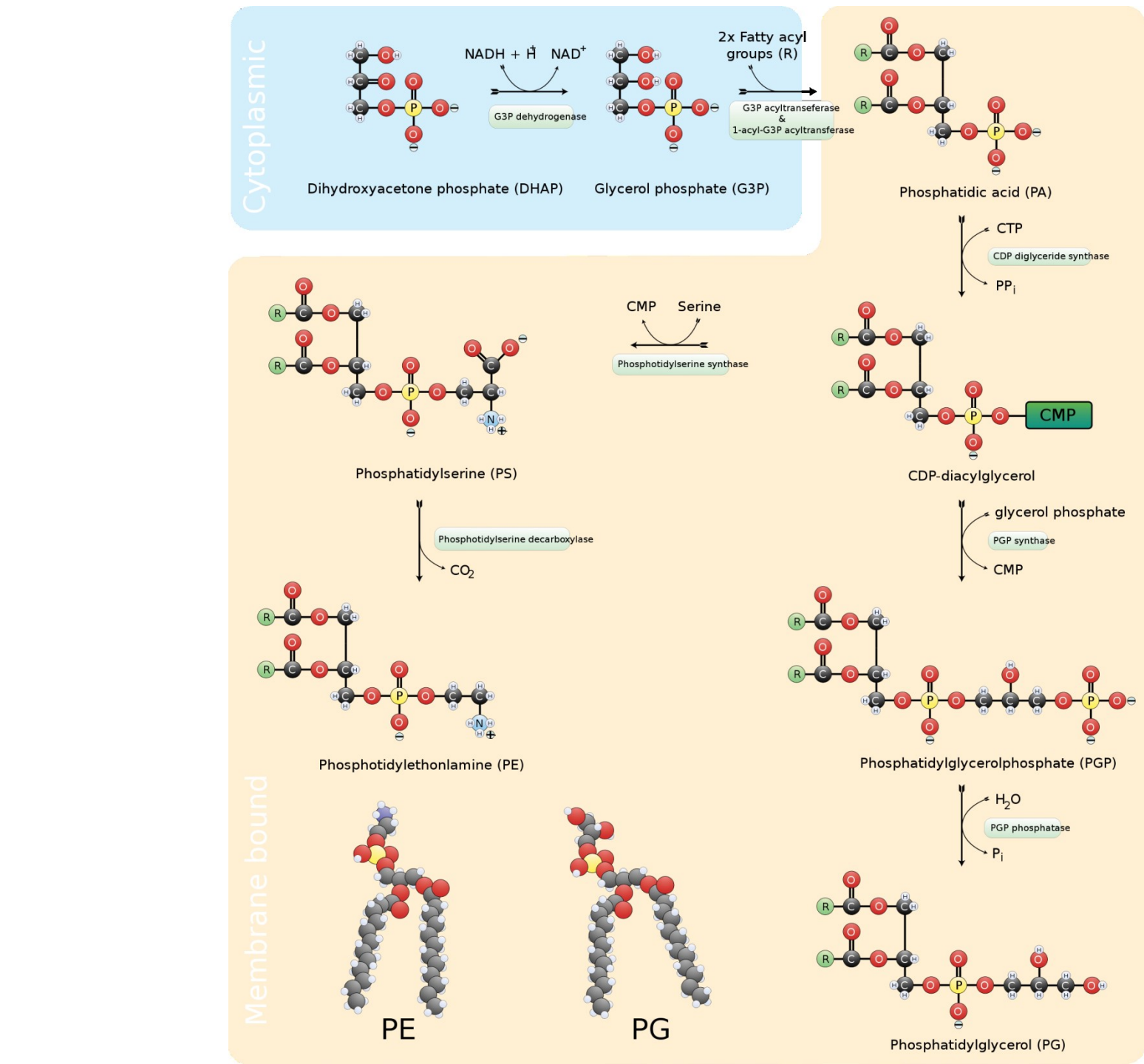
Cytoplasmic
NADH + H+
NAD+
G3P dehydrogenase
2x Fatty acyl groups (R)
G3P acyltransferase & 1-acyl-G3P acyltransferase
Dihydroxyacetone phosphate (DHAP)
Glycerol phosphate (G3P)
Phosphatidic acid (PA)
CTP
CDP diglyceride synthase
PPi
CMP
Serine
Phosphotidylserine synthase
Phosphatidylserine (PS)
CDP-diacylglycerol
Phosphotidylserine decarboxylase
CO2
glycerol phosphate
PGP synthase
CMP
Phosphotidylethonlamine (PE)
Phosphatidylglycerolphosphate (PGP)
Membrane bound
H2O
PGP phosphatase
Pi
PE
PG
Phosphatidylglycerol (PG)

Fusion proteins (SNARE)

SNARE proteins ("**SNA**P (Soluble NSF Attachment Protein) **RE**ceptor") are a large protein superfamily consisting of more than 60 members.

SNAREs can be divided into two categories:

vesicle or *v-SNAREs:* which are incorporated into the membranes of transport vesicles during budding.

target or *t-SNAREs:* which are located in the membranes of target compartments.

Although SNAREs vary considerably in structure and size, all share a segment in their cytosolic domain called a SNARE motif that consists of 60-70 amino acids and contains heptad repeats that have the ability to form coiled-coil structures.

V- and t-SNAREs are capable of reversible assembly into tight, four-helix bundles called "trans"-SNARE complexes.

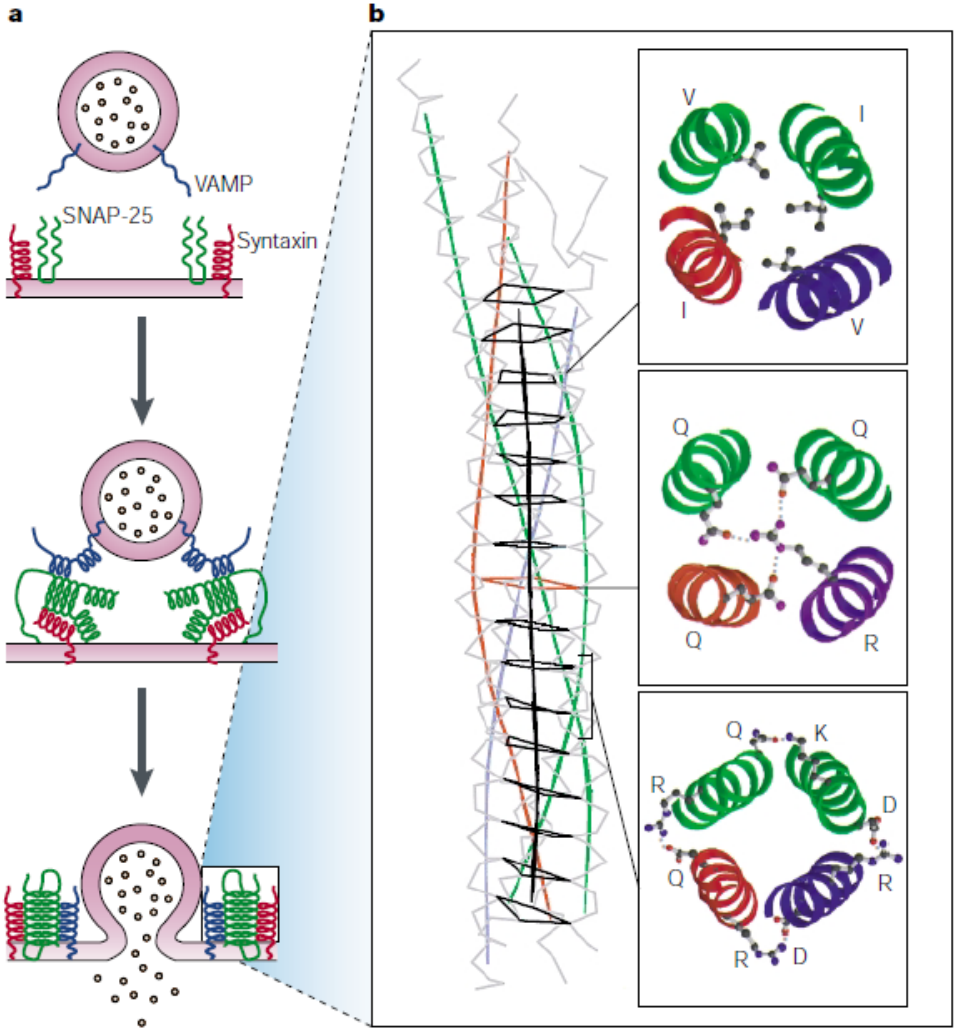

Figure 2 | **SNARE proteins form a four-helical bundle complex that drives membrane fusion**. **a** | VAMP (blue) on the vesicle interacts with syntaxin (red) and SNAP-25 (green) on the plasma membrane to form a four-helix bundle that zips up concomitant with bilayer fusion. **b** | The backbone of the SNARE complex is shown on the left[52], with the central ionic layer (red) and 15 hydrophobic layers (black) that mediate the core interactions highlighted. Top-down views of side-chain interactions are shown on the right, with the four SNARE helices shown as ribbons. The ball-and-stick structures represent the indicated amino acids; the dotted lines represent hydrogen bonds or salt bridges that stabilize interactions between SNAREs. Q-SNAREs and R-SNAREs are characterized by a glutamine (Q) or arginine (R) residue, respectively, in the central layer of the SNARE complex. (SNARE; soluble NSF attachment protein receptor, where NSF stands for *N*-ethyl-maleimide-sensitive fusion protein; SNAP-25, 25 kDa synaptosome-associated protein; VAMP, vesicle-associated membrane protein.)

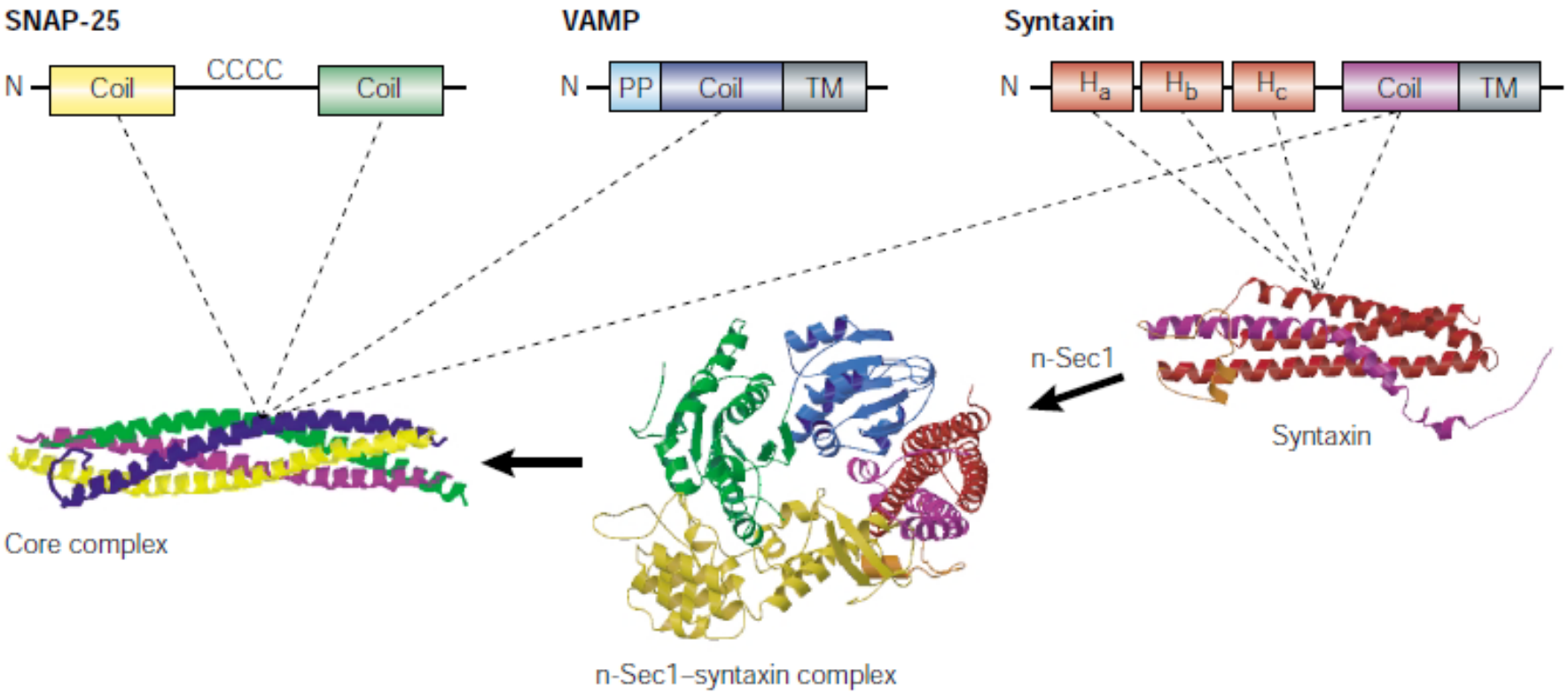

Figure 3 | **SNARE domain structures and the interaction between syntaxin and its chaperone protein n-Sec1.** The amino-terminal domain of syntaxin forms a three-helix bundle (red) that binds to its carboxy-terminal coil domain (purple), forming the closed conformation (right), which is bound and stabilized by n-sec1 (middle)[39]. A conformational change then occurs to allow dissociation of n-sec1 and the opening up of syntaxin, facilitating core complex formation. The coil domains of syntaxin, SNAP-25 and VAMP form the four-helix bundle core complex (left)[52]. In addition to the coil domain, VAMP harbours a proline-rich amino-terminal domain (PP) and SNAP-25 harbours a central domain that contains four palmitoylated cysteine residues (CCCC). (SNAP-25, 25 kDa synaptosome-associated protein; TM, transmembrane domain; VAMP, vesicle-associated membrane protein.)

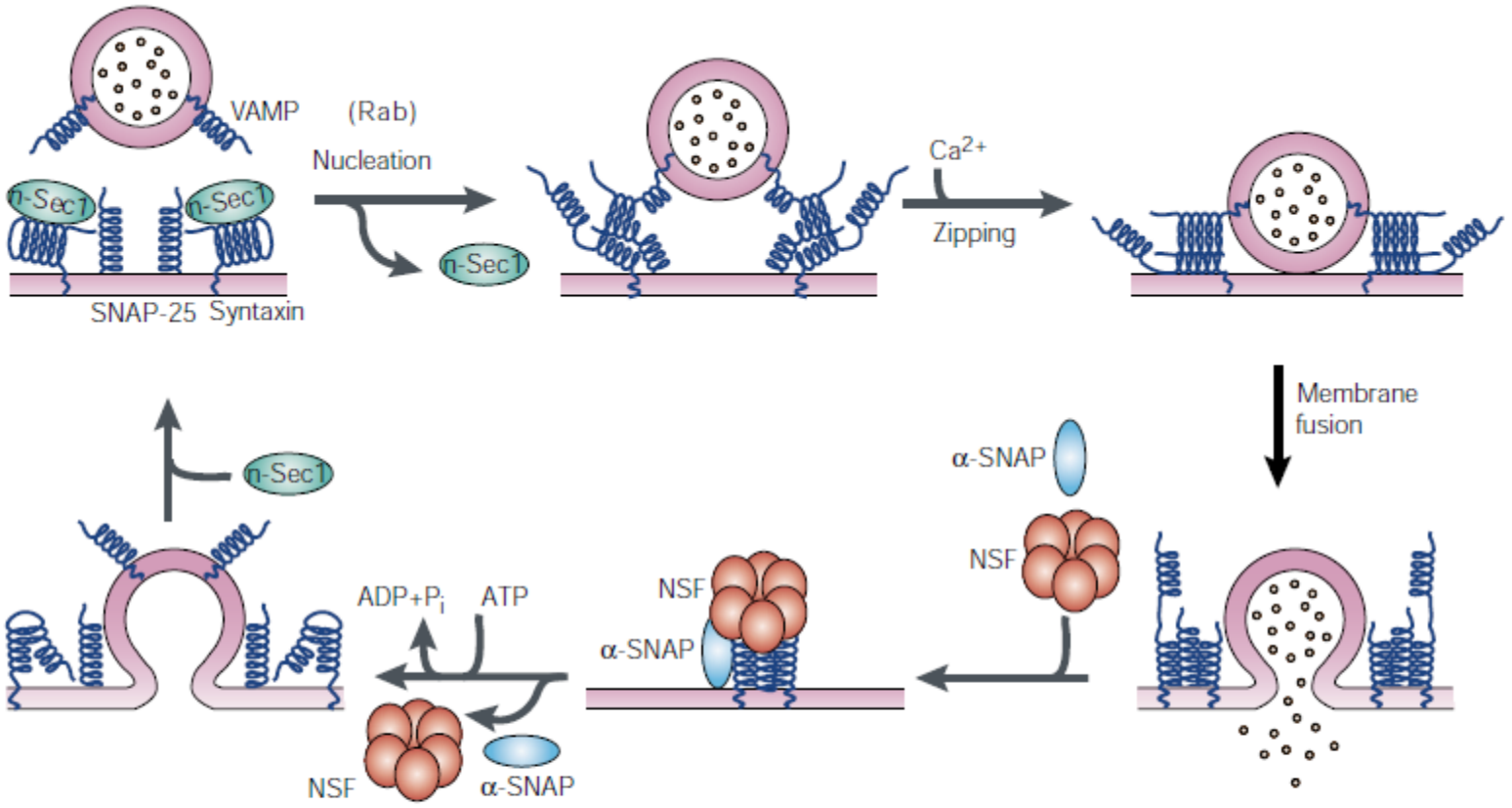

Figure 4 | **Molecular model of vesicle exocytosis**. Syntaxin is bound to n-Sec1 before formation of the core complex. Rab proteins might facilitate the dissociation of n-Sec1 from syntaxin, allowing subsequent binding (nucleation) between the three neuronal SNAREs, syntaxin, SNAP-25 and VAMP (for simplicity, only one coil is drawn for SNAP-25). Ca^{2+} triggers the full zipping of the coiled-coil complex, which results in membrane fusion and release of vesicle contents. After the fusion event, recruitment of α-SNAP and NSF from the cytoplasm and subsequent hydrolysis of ATP by NSF causes dissociation of the SNARE complex. Syntaxin, VAMP and SNAP-25 are then free for recycling and another round of exocytosis. (NSF; *N*-ethyl-maleimide-sensitive fusion protein; SNAP-25, 25 kDa synaptosome-associated protein; SNARE, soluble NSF attachment protein receptor, VAMP, vesicle-associated membrane protein.)

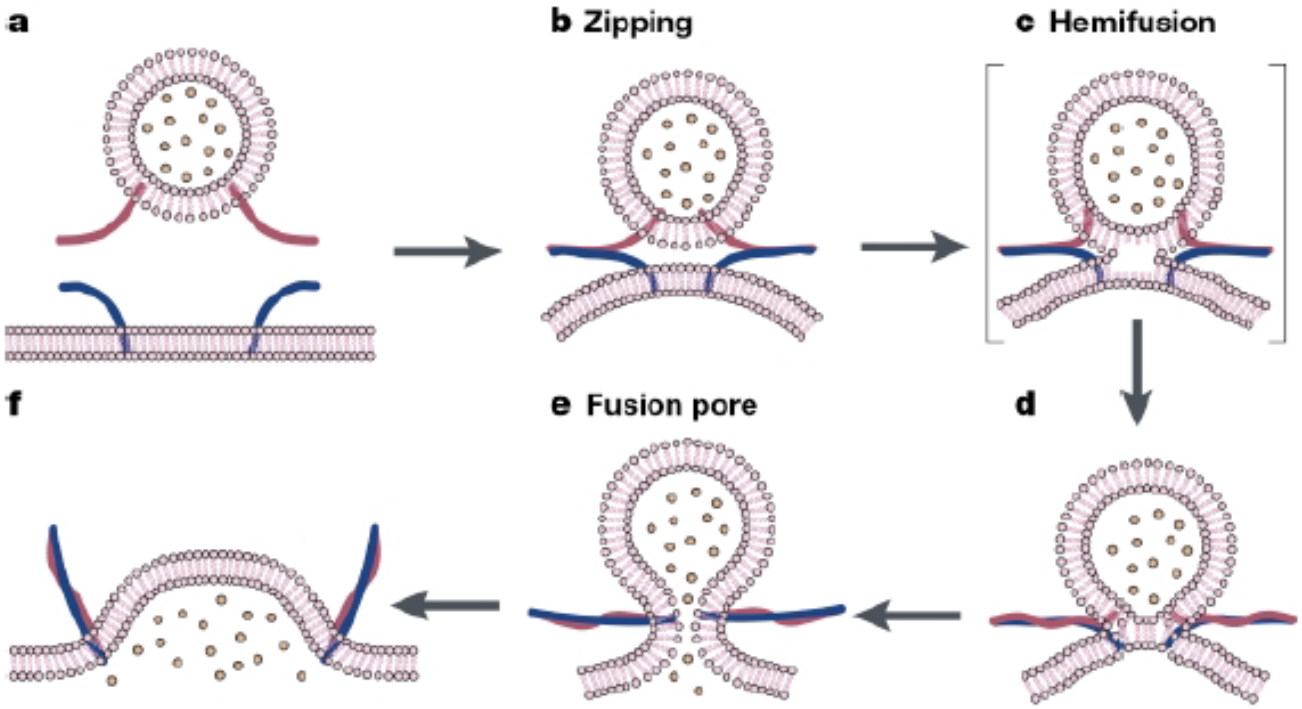

Figure 5 | **Model of SNARE-mediated lipid fusion. a** | The two membranes are in the vicinity of each other but the SNAREs are not yet in contact. **b** | SNARE complexes start zipping from the amino-terminal end, which draws the two membranes further towards each other. **c** | Zipping proceeds, causing increased curvature and lateral tension of the membranes, exposing the bilayer interior. Spontaneous hemifusion occurs as the separation is sufficiently reduced. **d** | The highly unfavourable void space at the membrane junction in (**c**) causes the establishment of contacts between the distal membrane leaflets. **e** | The lateral tension in the transbilayer contact area induces membrane breakdown, yielding a fusion pore. **f** | The fusion pore expands and the membrane relaxes. (SNARE, soluble NSF attachment protein receptor, where NSF stands for *N*-ethyl-maleimide-sensitive fusion protein.)

Membrane dynamics in gametes

Membrane asymmetry

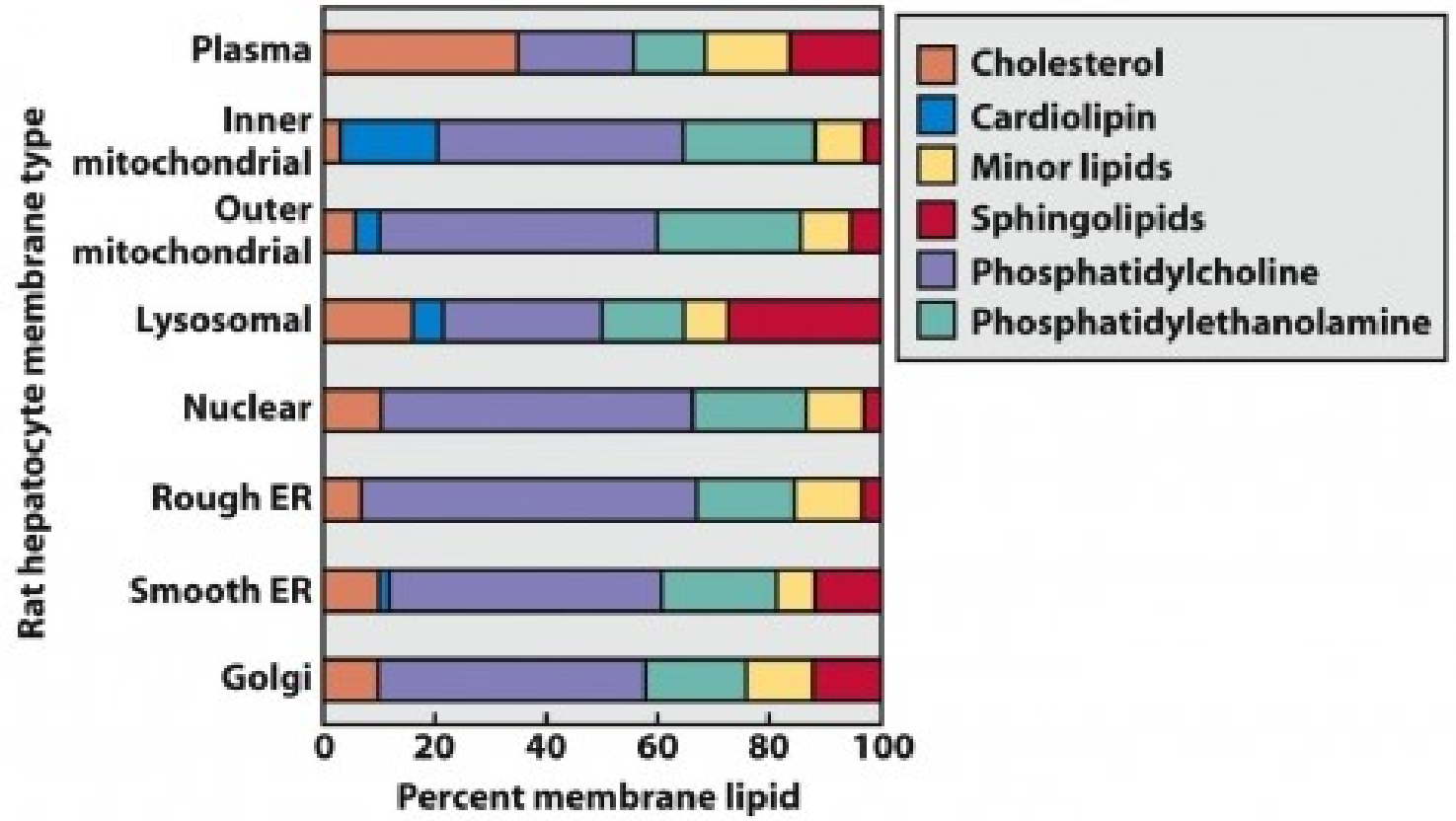

Figure 11-2
Lehninger Principles of Biochemistry, Fifth Edition

Membrane asymmetry

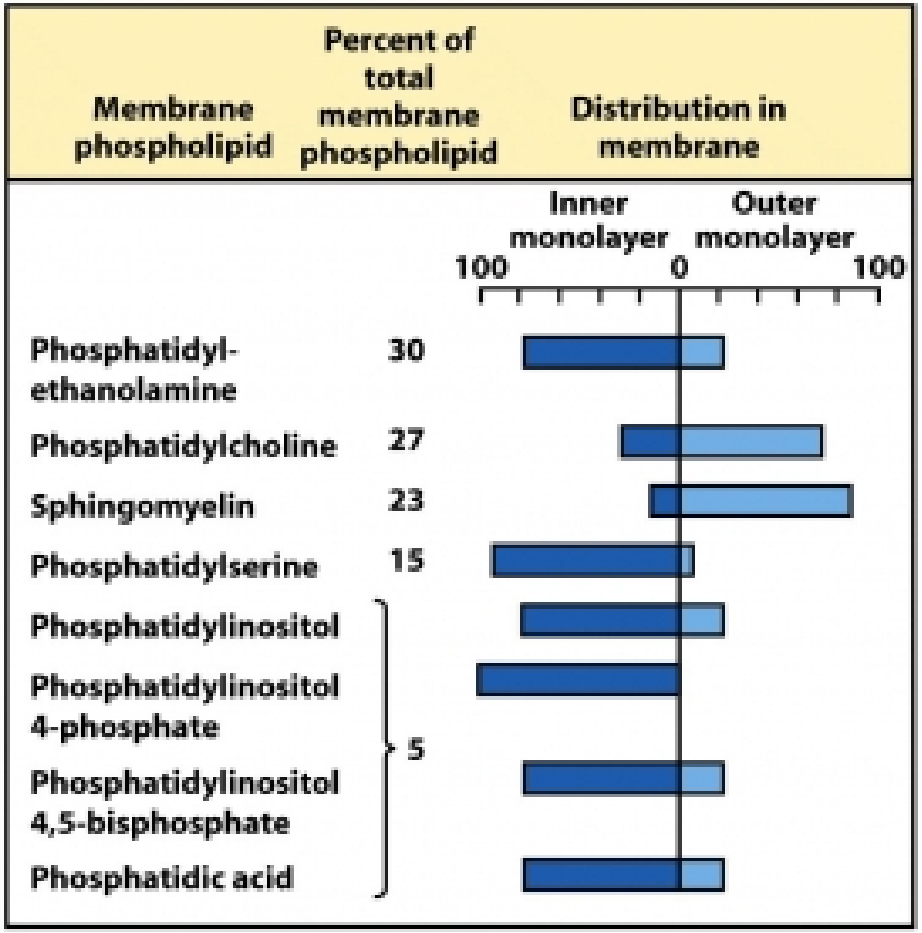

Figure 11-5
Lehninger Principles of Biochemistry, Fifth Edition

Membrane asymmetry

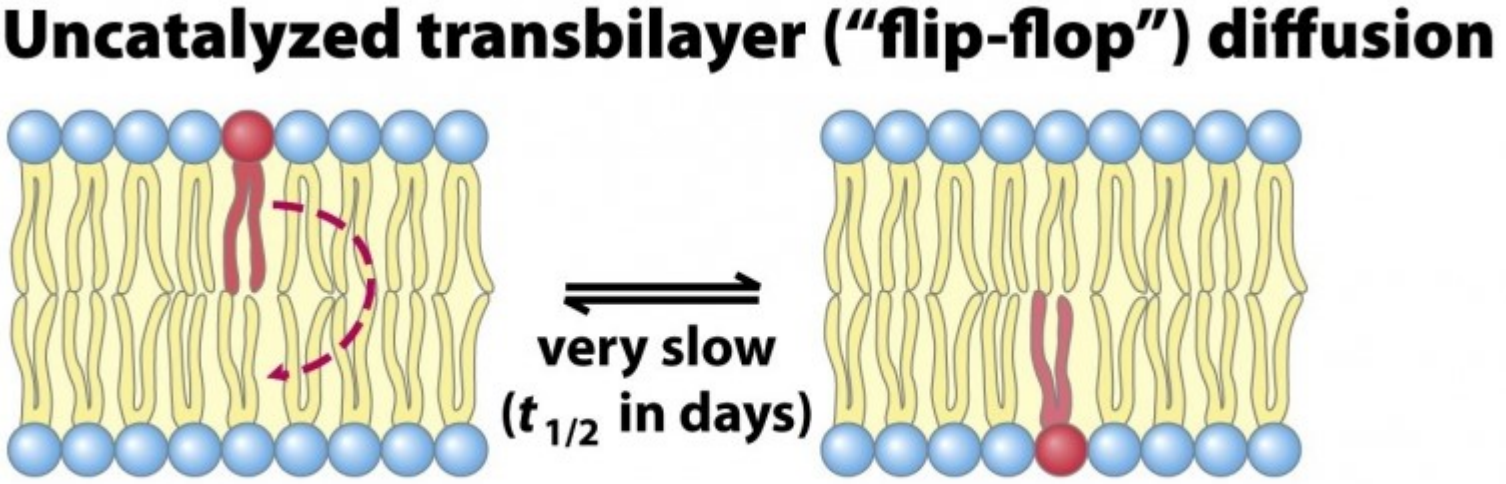

Figure 11-16a
Lehninger Principles of Biochemistry, Fifth Edition

Enzymes and membrane asymmetry

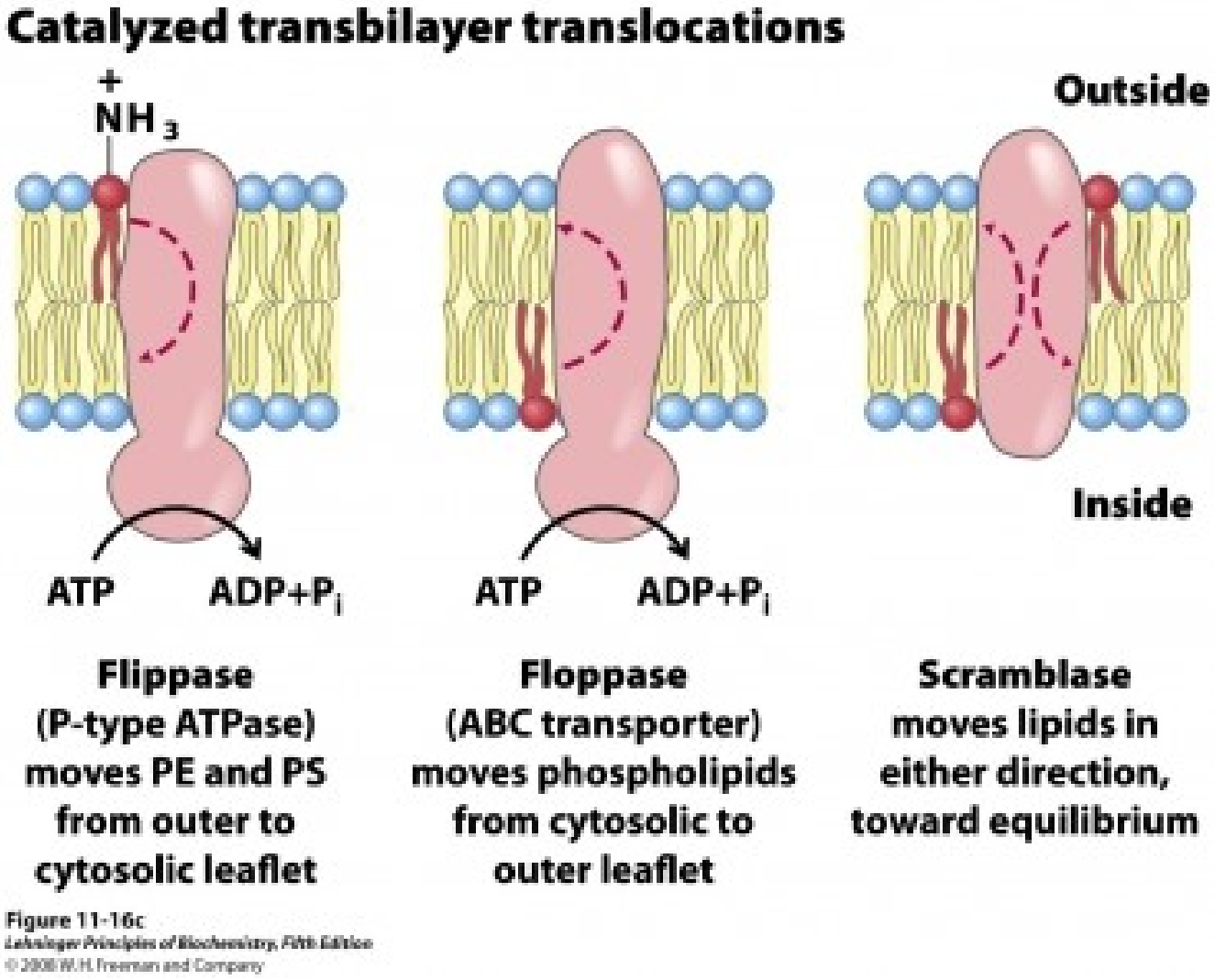

Figure 11-16c
Lehninger Principles of Biochemistry, Fifth Edition

ASIMMETRIA di MEMBRANA

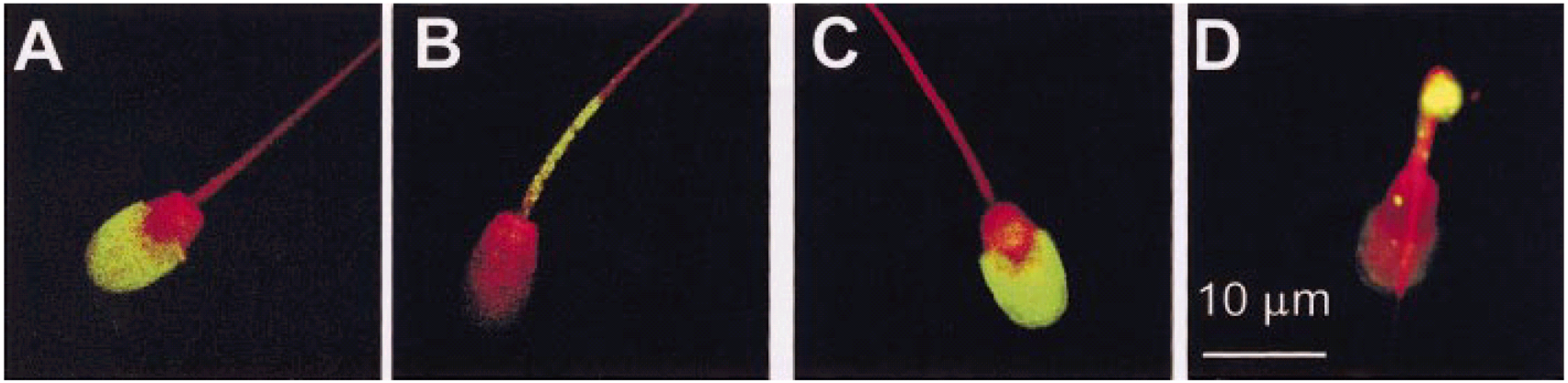

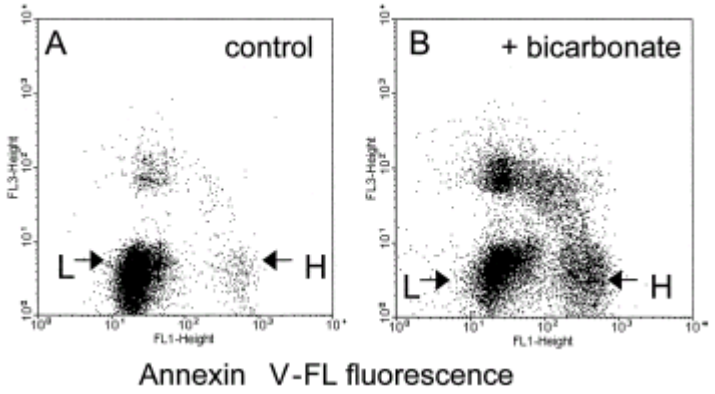

Spermatozoa were incubated in HBT-Bic for 2h and then stained with annexin V-FL (green) to detect exposed PS (**A** and **B**) or with Ro-SA-FL (green) to detect exposed PE (**C** and **D**), all cells were counterstained with 0.1 mM C6LRh (hexanoic acid conjugated to lissaminylrhodamine) to label the entire plasma membrane red.

*Gadella and Harrison, BOR **67,** 340–350 (2002)*

Membrane domains

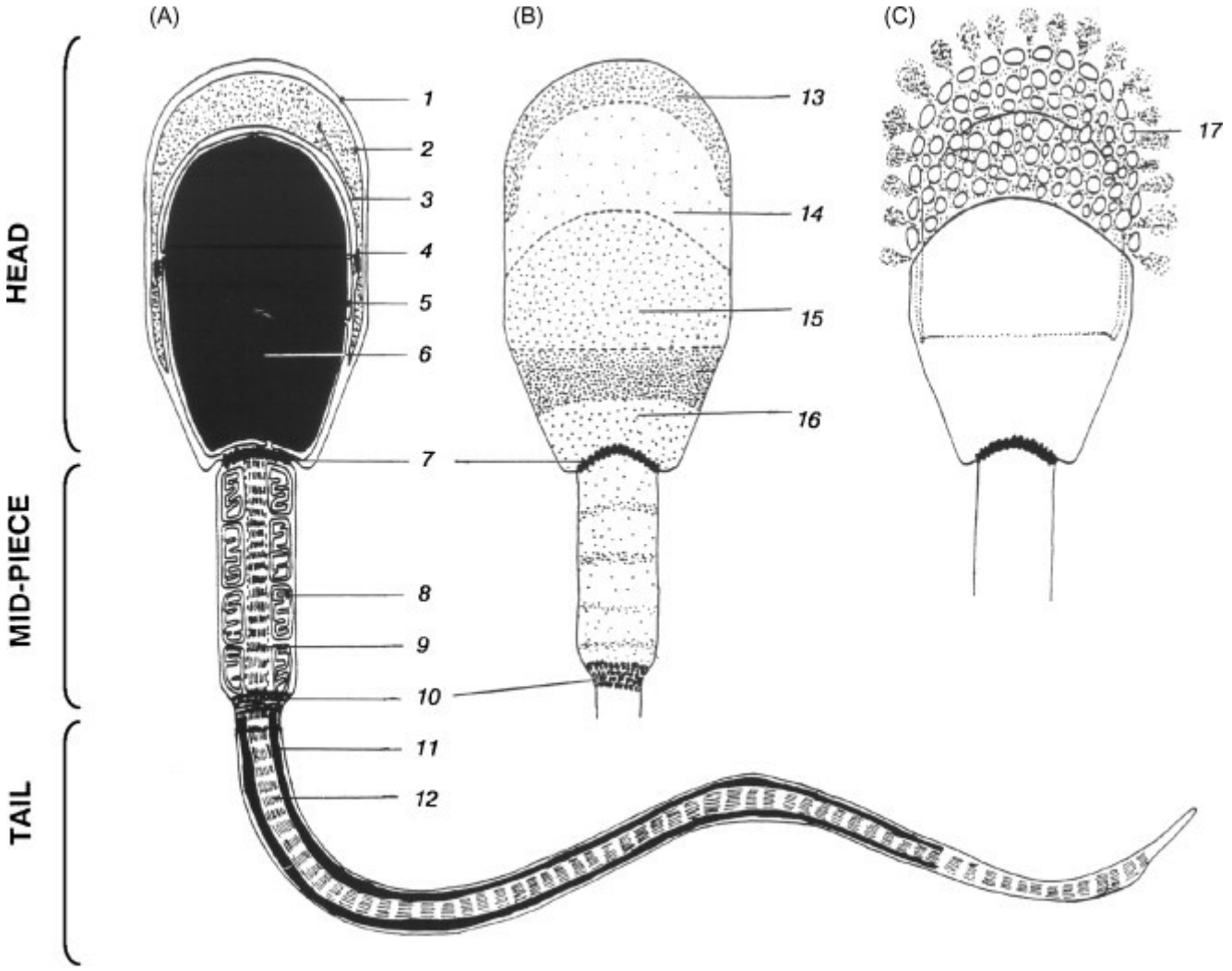

Domains: structure

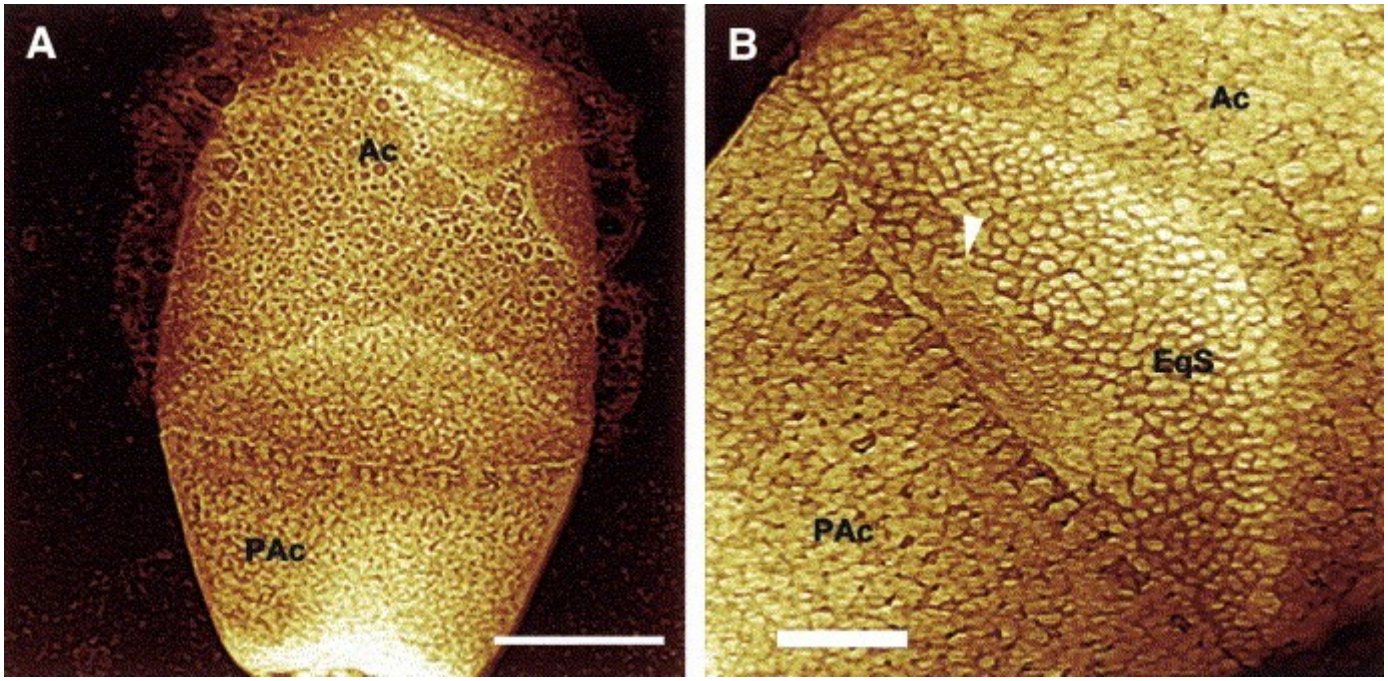

Domains: function

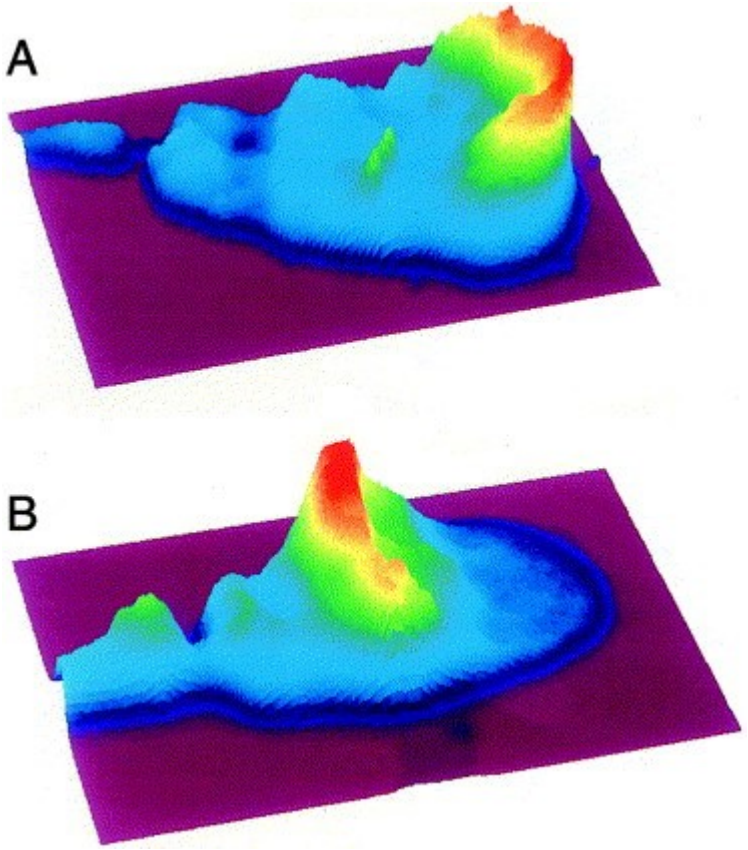

Fusogenicity

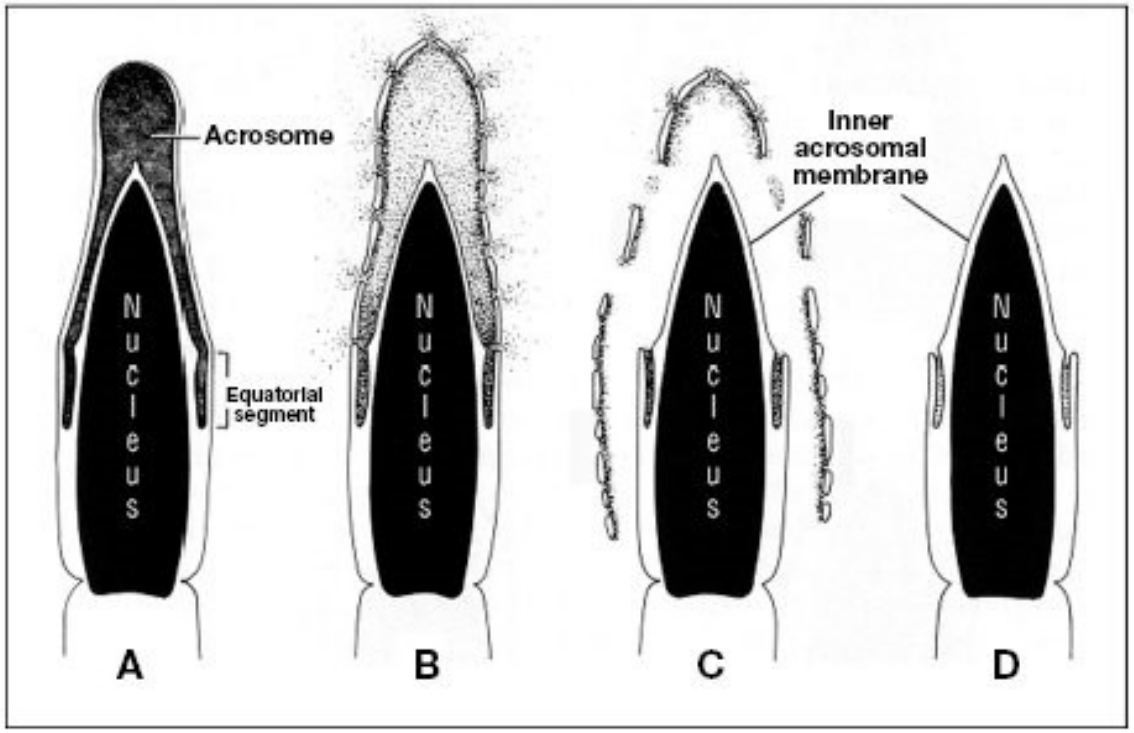

MC540

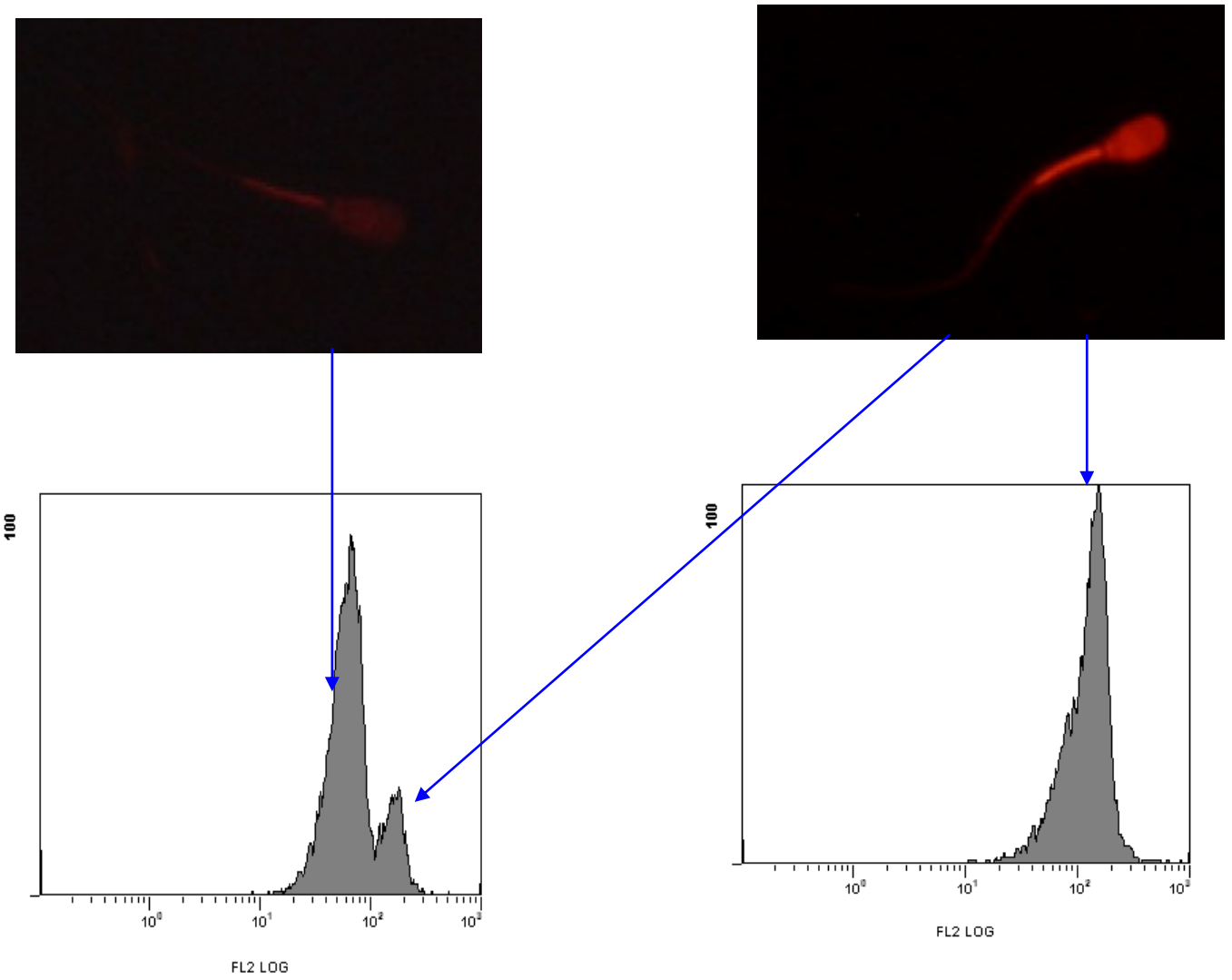

FILIPIN

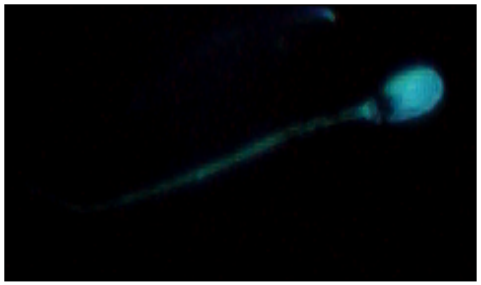

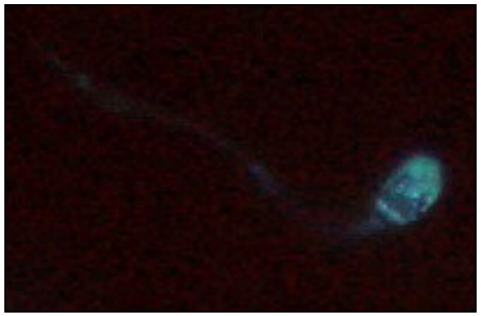

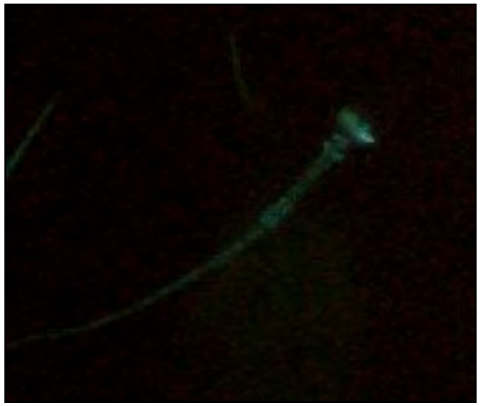

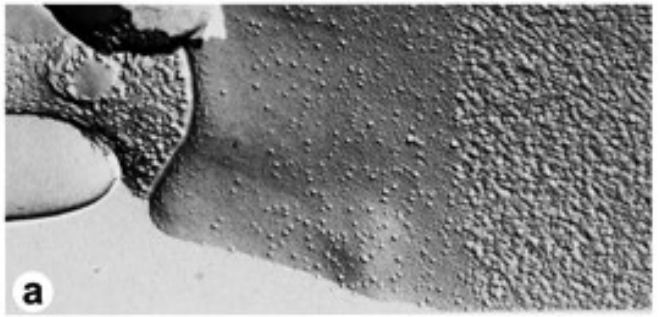

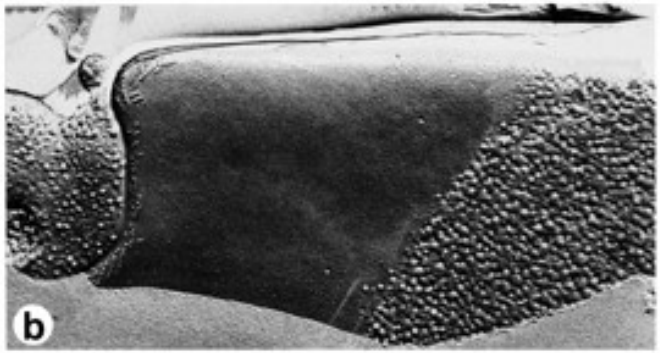

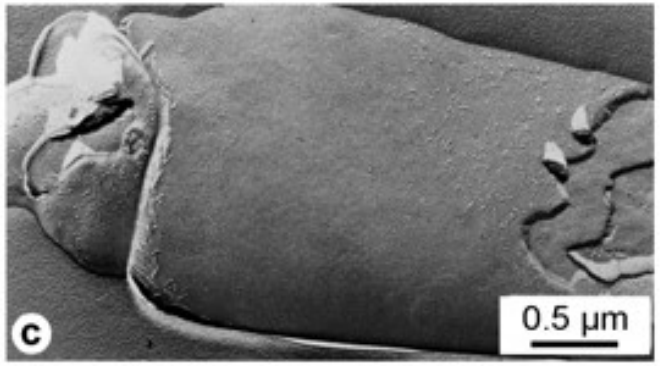

FRAP

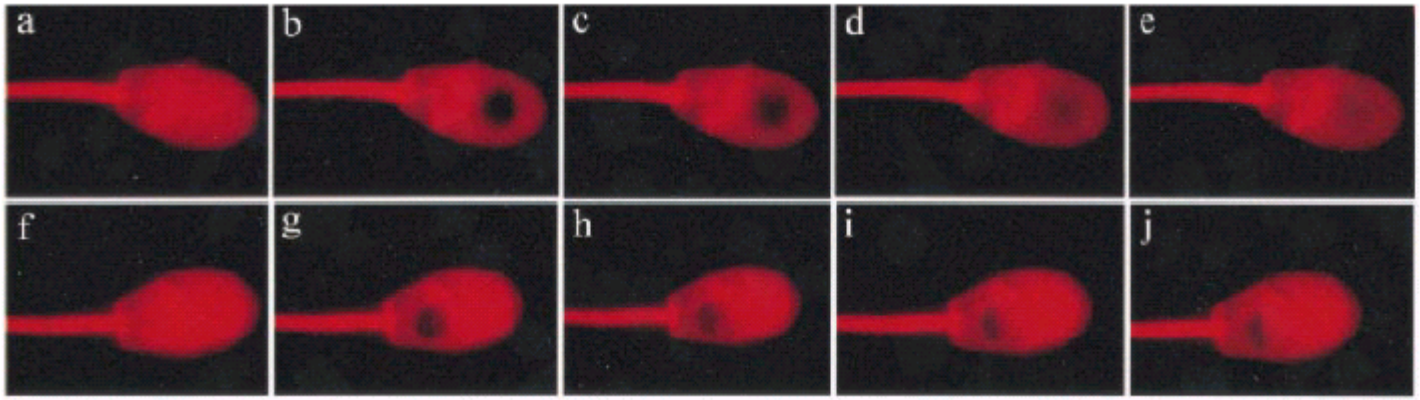

Spermatozoa stained with DiIC12 and subjected to large-area photobleaching: **a** and **f**) spermatozoa before photobleaching; **b**–**e**) the focused laser beam has been centered over the acrosome, followed by photobleaching.

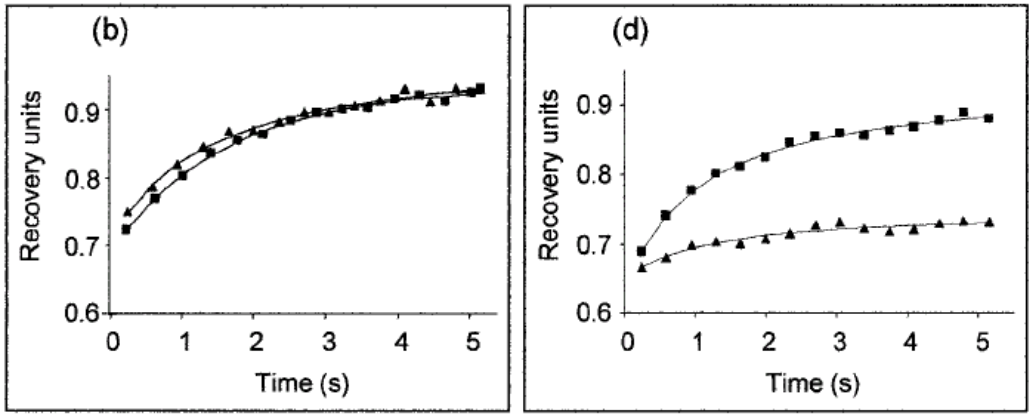

*Mackie et al., BOR **64,** 113–119 (2001)*

LAURDAN (ordine)

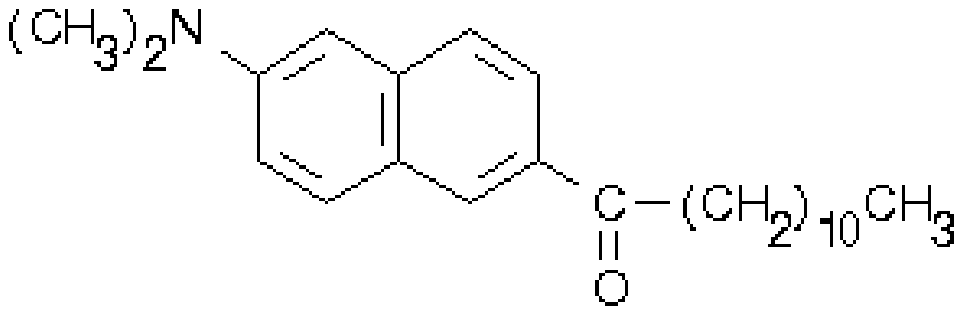

$$GP_{Laurdan} = \frac{I_{440} - I_{490}}{I_{440} + I_{490}}$$

LAURDAN (anisotropy)

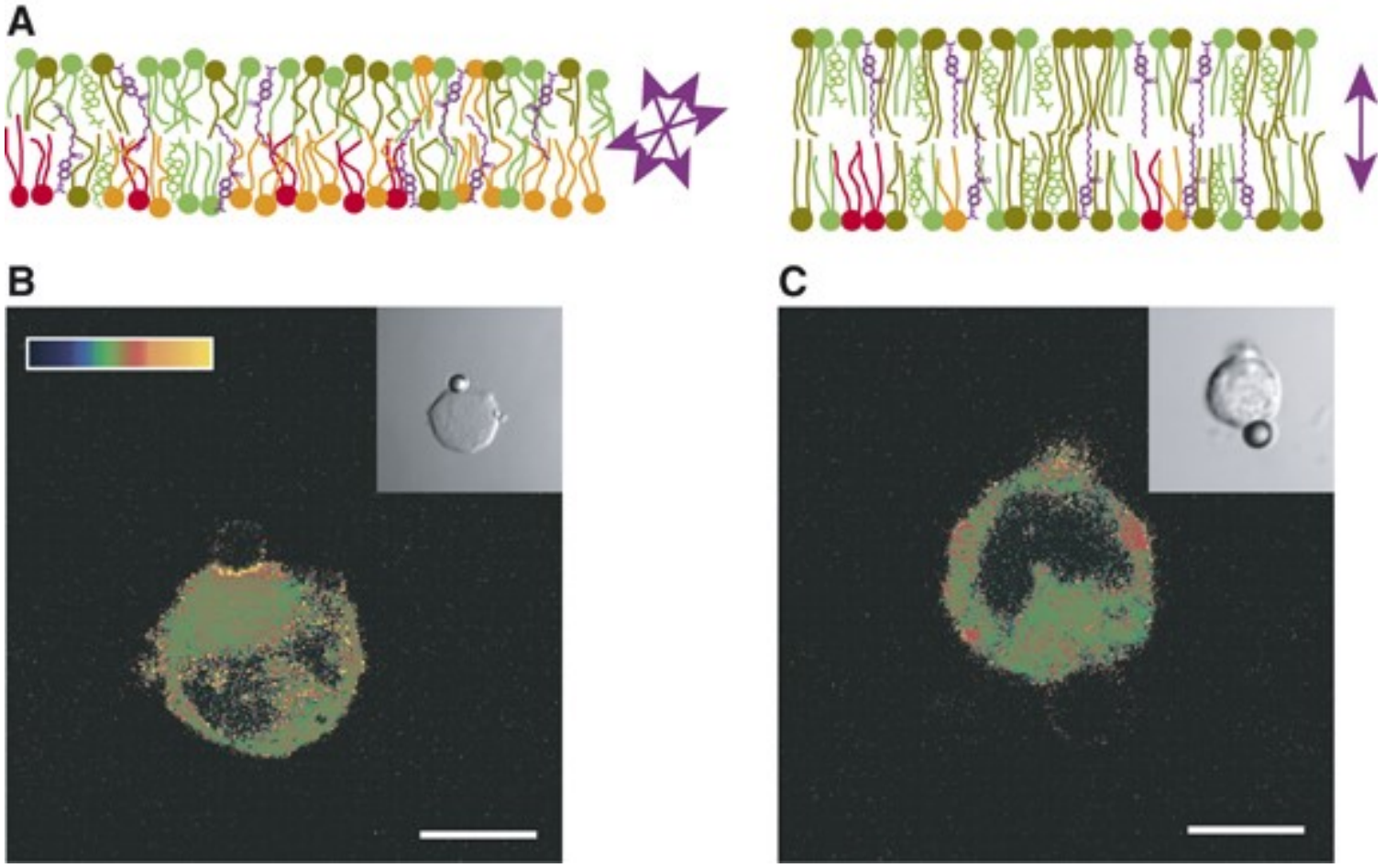

CTC staining

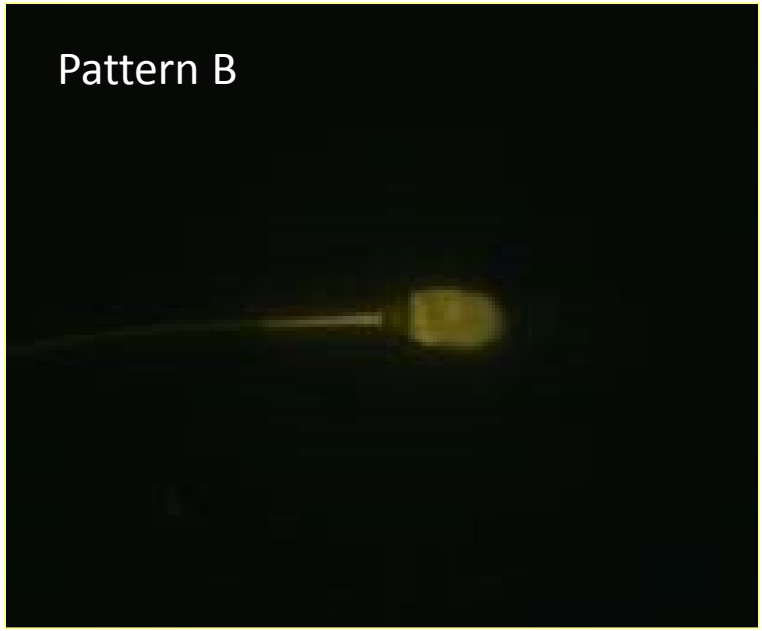

- empirica
- rapida

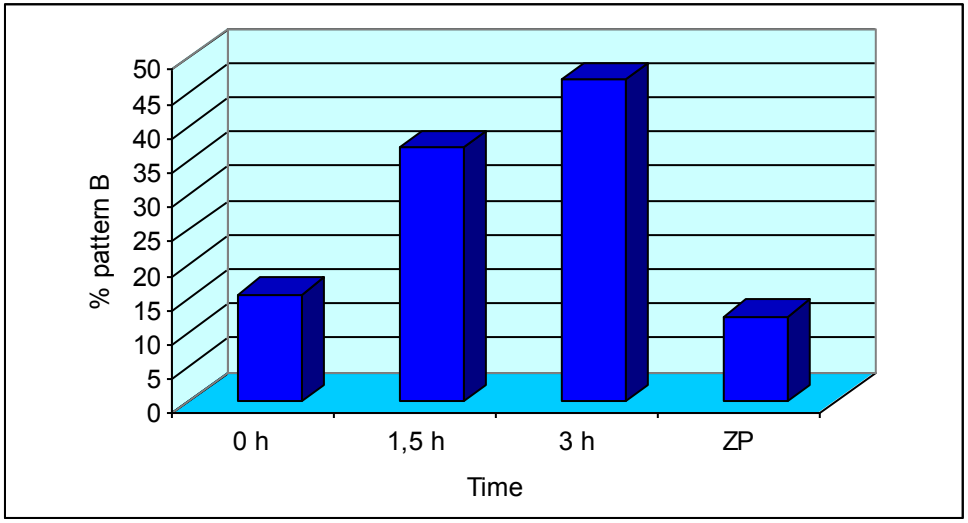

Mattioli et al, …. (1996)

CTC

uncapacitatided

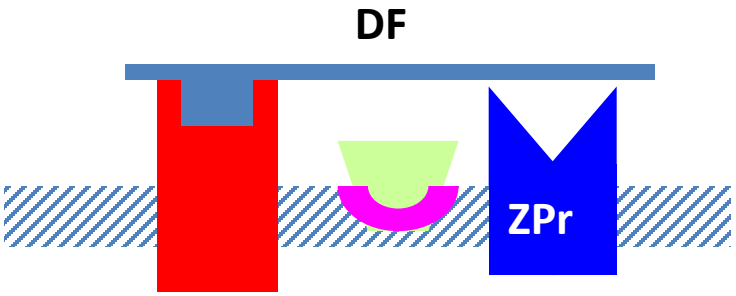

capacitatided

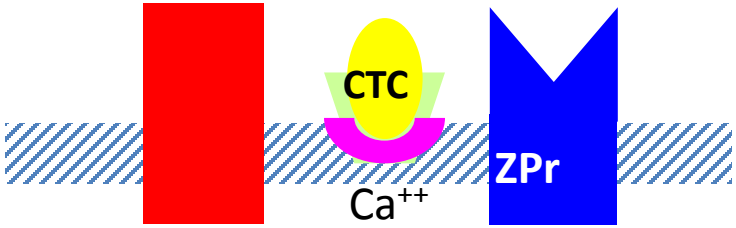

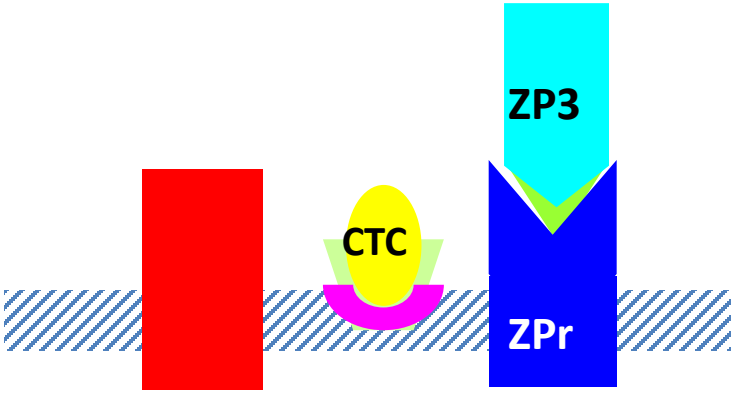

acrosomal reaction

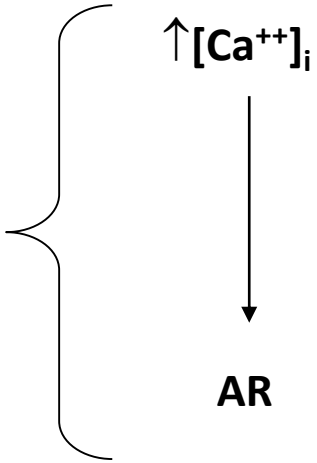

CONTROLLO: cAMP

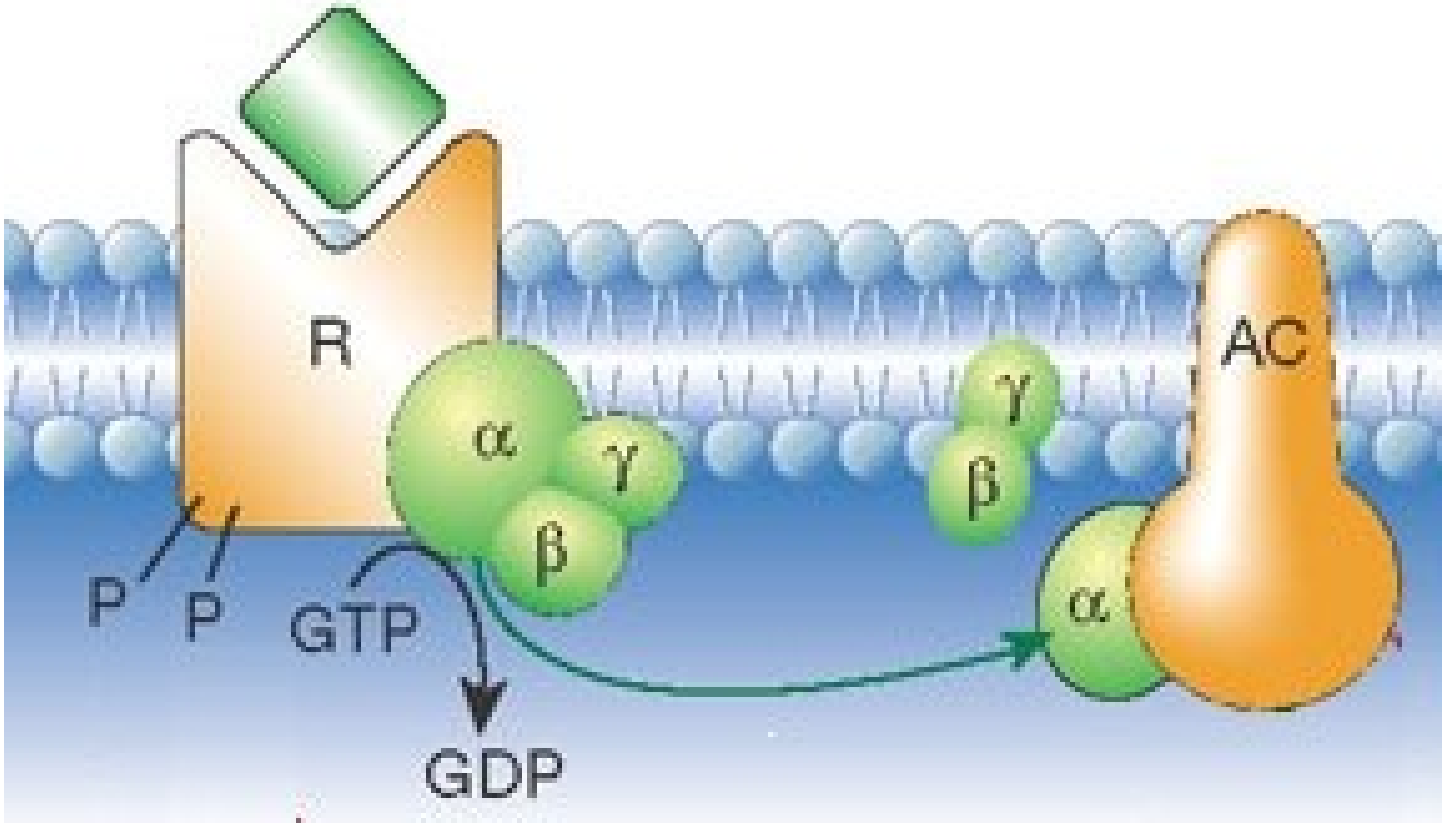

cAMP

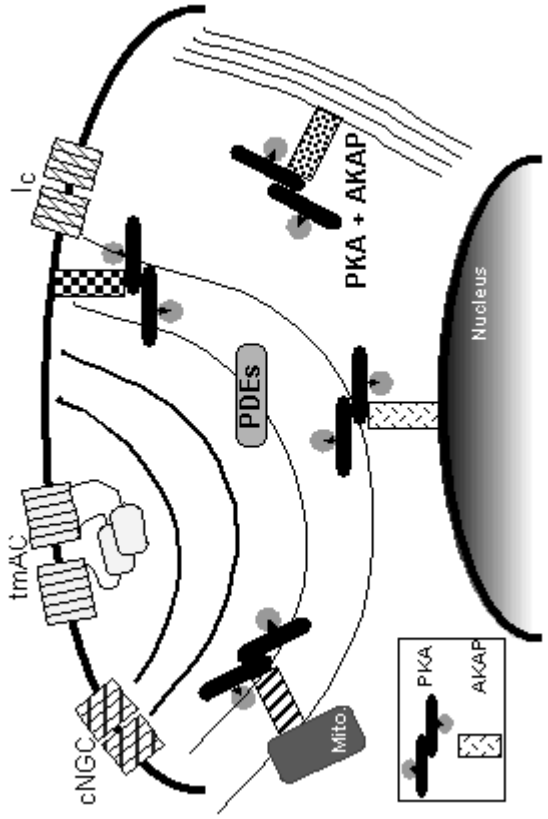

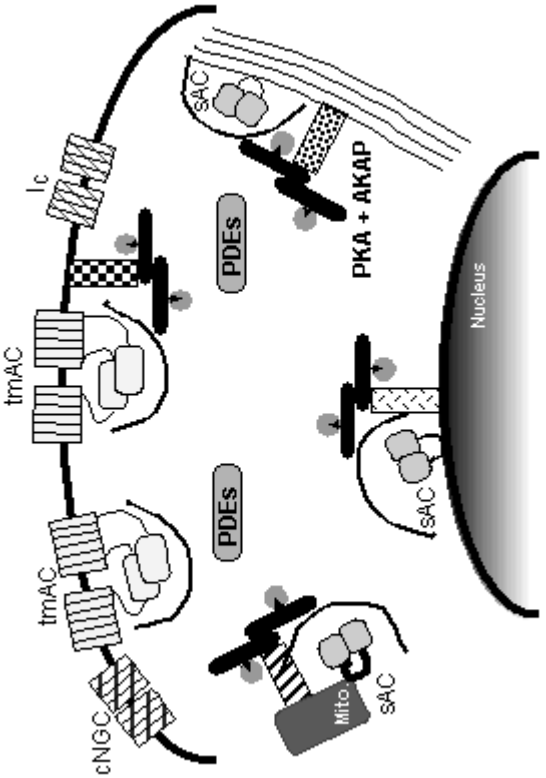

ISOFORM		SIZE	ACTIVITY
sAC_{fl}	C1 C2 P L-Zip	187 Kd	1X
sAC_t	C1 C2	~50 Kd	20X

BICARBONATE

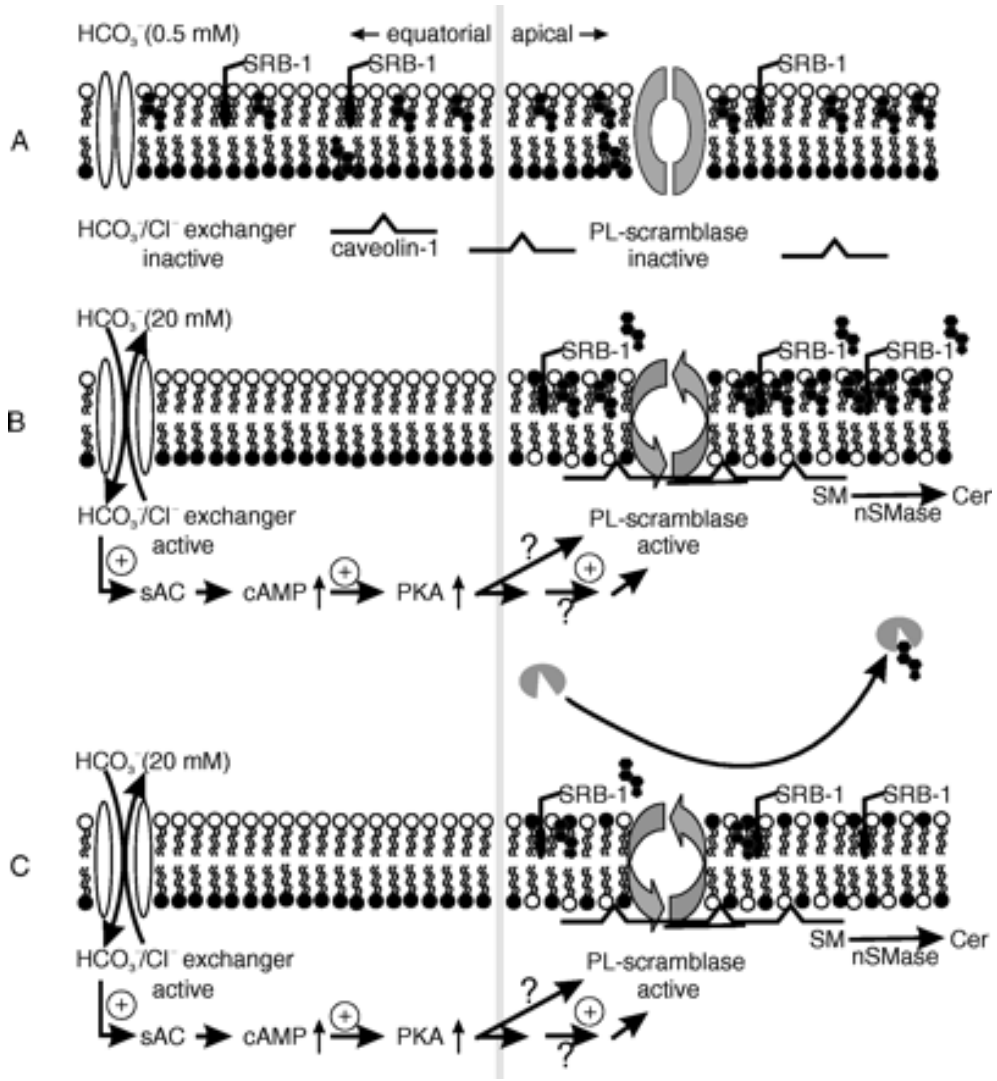

BICARBONATE

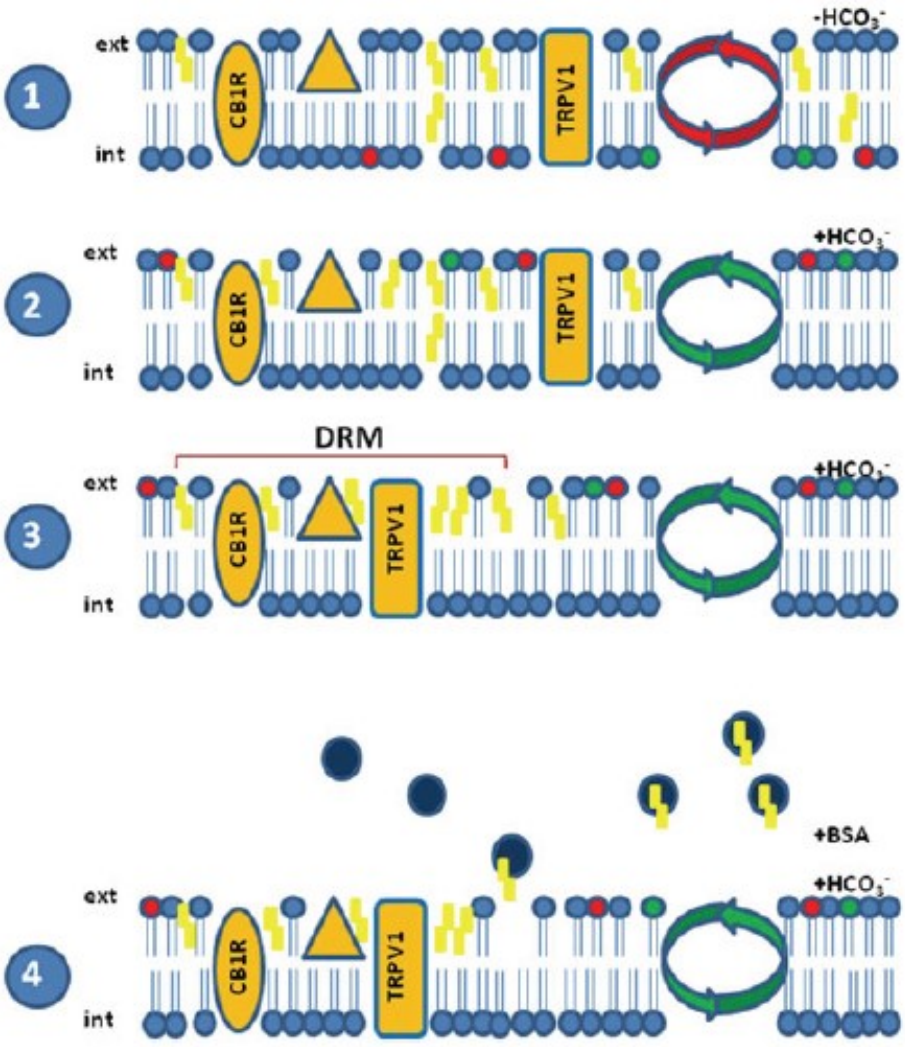

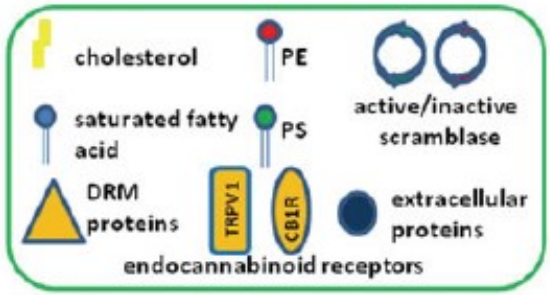

The HCO3- promotes the activation of scramblase.

The DRMs associate and their composition in proteins changes; the signalling machinery reorganizes.

The extracellular proteins extract cholesterol from membranes